STABLE ISOTOPE PARTITIONING OF EVAPOTRANSPIRATION ACROSS A SHRUB-GRASS ECOTONE FOLLOWING A PRECIPITATION EVENT SEVILLETA NATIONAL WILDLIFE REFUGE, USA

by

John Robert Boulanger

Submitted in partial fulfillment

of the requirements for the degree of

Master of Science in Hydrology

New Mexico Institute of Mining and Technology

Department of Earth and Environmental Science

Socorro, New Mexico

May 2004

ABSTRACT

The Sevilleta National Wildlife Refuge (SNWR) in central New Mexico exhibits the widespread shrub encroachment onto former semiarid grasslands that is common throughout the southwestern United States. Many factors, such as fire suppression and high levels of herbivory, have been suggested causes for the widespread shrub encroachment. The encroachment may be related to alternate factors, since it has continued in the SNWR to the present day despite a lack of fire suppression and high levels of herbivory for nearly half a century. Current research in the SNWR evaluates plant response to drought. The results provide evidence that water cycling plays a role in the advancement of shrubs onto grasses. To address wet-season water cycling, the evaporation (E) and transpiration (T) rates were estimated for the shrub and grass ecosystems in the SNWR following a precipitation event. The plant with the higher T rate limits the availability of soil water to the competing plant and the former plant population will likely increase and expand.

Soil samples were collected from both the shrub ecosystem and the grass ecosystem. For both ecosystems, samples were obtained from control (unaltered) and treatment (no transpiration) plots along a shrub-grass ecotone in the SNWR before, immediately after and for six consecutive days following a wet-season precipitation event. Samples were selected by means of a random sampling procedure. The soil samples were analyzed for stable isotope ($\delta^{18}O$ and $\delta^{2}H$) composition and water content.

Given the removal of plants and thus transpiration from the treatment plots, the E rate from the treatment plots was expected to be higher than the E rate from the control plots. The treatment plots have more soil water available for evaporation since T is absent. As the soil water content decreases, the E rate decreases. The treatment plot soil waters for both ecosystems were expected to show more stable isotope enrichment and a higher water content than control plot soil waters. Transpiration (or soil water extraction by plants) has been shown to be non-fractionating. It was then assumed that T would not influence the soil water stable isotope signature that results from evaporation.

The treatment plot soil waters showed more stable isotope enrichment and higher water content than the control plot soil waters. A stable isotope balance model was necessary to quantitatively estimate the evaporation and transpiration rates for each ecosystem. The results of this study will demonstrate that transpiration affects the amount of soil water available for evaporation, and therefore influences the extent of stable isotope fractionation. The model results show that the evaporation rate from the treatment plots was higher than the control plots for both ecosystems. The water content, however, remained higher in the treatment plots because the control plots had additional soil water loss due to transpiration. The level of stable isotope enrichment does not depend only on total soil water loss. The greater level of stable isotope enrichment in the treatment plots is due to the fraction of soil water loss by evaporation being greater in the treatment plots than the control plots.

Of the total post-precipitation soil water loss in the shrub ecosystem, 16-21% was transpired by the shrubs and 79-84% was evaporated. Of the total post-precipitation soil water loss in the grass ecosystem, 30-48% was transpired by the grasses and 52-70% was evaporated. Six days after the precipitation event, these figures translate into 9.0 to 13 mm of soil water transpired by the grasses, while the shrubs transpired 7.5 to 9.0 mm of soil water. This study shows that the shrubs do not have an advantage over grasses, with respect to removing soil moisture that infiltrates following a typical wet-season precipitation event. Additional work is necessary to assess how the contrasts in water use between grasses and shrubs varies throughout the year, and how this contributes to the long term changes in ecosystem structure associated with the shrub encroachment.

DEDICATION

To my Wife and Angel, Maggie.

To my Father for having Her Heaven sent.

ACKNOWLEDGEMENTS

I thank Dr. Eric Small from the University of Colorado, Boulder for his support of this study and willingness to accommodate my research interests. Dr. Campbell for his support and advice at both committee meetings and guidance in the laboratory. Dr. Phillips for his guidance during the development of the stable isotope balance model and his support and advice at both committee meetings. Dr. Aitbayev, Dr. Stone and Randy Roberts for their time and support during the development of the stable isotope balance model. Dr. Ballou for her assistance with ANOVA statistics.

I would especially like to thank my wife, Maggie Boulanger, and fellow students, Aaron Abel, David Boutt, Huade Guan, Gabrielle Kurth, Mike Ranck, Peter Stone and David Yin for their devotion as field assistants at 4am. THANK YOU!

I am indebted to Johnnie Lyman and Karen Hickey for their generous assistance on many occasions during the lab stage of my research. I'm not in the doghouse anymore!

My fellow research group members, Eric Bhark, Jim Elliott, Shirley Kurc and Douglas McGhee, Amber Owings, and Andrew Phillips assisted numerous group research efforts. Despite occasional bickering under the hot desert sun, we certainly accomplished many, many nearly impossible tasks. Thanks for your help.

TABLE OF CONTENTS

LIST OF TABLES

LIST OF FIGURES

Figures

Page

1. INTRODUCTION

The Sevilleta National Wildlife Refuge (SNWR) (**Figure 1.1**) provides a natural laboratory for the study of ecosystems. The SNWR is restricted to public access; therefore the ecosystems function in an undisturbed (no human intervention) environment. Four biomes currently coexist within the SNWR: Great Plains Grassland, Great Basin shrub-steppe, Chihuahuan Desert and Montane Coniferous Forest (**http://sevilleta.unm.edu**). This study addresses the encroachment of Great Basin shrub-steppe ('shrub(s)' or 'shrub ecosystem') onto Chihuahuan Desert grasses ('grass(es)' or 'grass ecosystem') in the SNWR (**Figure 1.2**). Similar encroachments have been documented throughout the southwestern United States (**Buffington and Herbel, 1965, Hennessy et al., 1983, & York and Dick-Peddie, 1969**). The principal species include *Larrea tridentata* or creosotebush (shrub) and *Bouteloua eriopoda* or black-grama grass (grass).

Many factors, such as fire suppression and high levels of herbivory, have been suggested causes for the widespread shrub encroachment onto former semiarid grasslands that is common throughout the southwestern United States (**Neilson, 1986; Bahre, 1991; Inglis, 1964; Humphrey, 1958**). The encroachment may be related to alternate factors, since it has continued in the SNWR to the present day despite a lack of fire suppression and high levels of herbivory for nearly half a century (**http://sevilleta.unm.edu**). Current research in the SNWR evaluates plant response to drought (**Weltzin et al., 2003; Small and Kurc, 2003**). The results provide evidence that water cycling plays a role in the advancement of shrubs onto grasses in the SNWR. **Schlesinger et al., 1990** in the Jornada Experimental Range in southern New Mexico, also demonstrated the importance of water cycling in the advancement of shrubs onto grasses. To address wet-season (July to October) water cycling, the evaporation (E) and transpiration (T) rates were estimated in this study for the shrub and grass ecosystems in the SNWR following a precipitation event. The grasses only transpire during the wet-season. The plant with the higher T rate limits the availability of soil water to the competing plant (**Bhark, 2002; Bhark and Small, 2003**) and the former plant population will likely increase and expand.

Soil samples were collected from both the shrub ecosystem and the grass ecosystem. For both ecosystems, samples were obtained from control (unaltered) and treatment (no transpiration) plots along a shrub-grass ecotone in the SNWR before, immediately after and for six consecutive days following a wet-season precipitation event. Samples were selected by means of a random sampling procedure. All soil samples were analyzed for water content. The soil waters collected before the storm (Day –X[1]), immediately after the event (Day 0), and two (Day 2) and six (Day 6) days after the event were analyzed for $\delta^{18}O$ composition. Day 0 and Day 6 soil waters were also analyzed for $\delta^{2}H$ composition.

Given the removal of plants and thus transpiration from the treatment plots, the E rate from the treatment plots was expected to be higher than the E rate from the control plots. The treatment plots have more soil water available for evaporation since T is absent. As the soil water content decreases, the E rate decreases (**Hornberger et al., 1998**). The treatment plot soil waters for both ecosystems were expected to show more stable isotope enrichment and a higher water content than control plot soil waters.

[1] Pre-event soil samples and lab records (Appendix I: Data) designated 'Day –X'. The number of days prior to the event was unknown during collection. The actual number of days prior to the event is two.

However, it could not be anticipated if the E flux from the treatment plot would be less than the combined flux of E and T from the control plots. Transpiration (or soil water extraction by plants) has been shown to be non-fractionating (**Zimmerman et al., 1967**). It was then assumed that T would not influence the soil water stable isotope signature that results from evaporation. Through stable isotope mass balance on soil water, the evaporation rate could be estimated (**Barnes and Allison, 1983**) and then the T rate could be inferred through a mass-balance comparison of the control and treatment plots.

The treatment plot soil waters showed more stable isotope enrichment and higher water content than the control plot soil waters. A stable isotope balance model was necessary to quantitatively estimate the evaporation and transpiration rates for each ecosystem. A recent study attempted to partition evapotranspiration (ET) into its two components, evaporation and transpiration (**Hsieh et al., 1998**). The authors assumed stable isotope fractionation depended solely on the degree of evaporation. This assumption is an over-simplification. The results of this study will demonstrate that transpiration affects the amount of soil water available for evaporation, and therefore influences the extent of stable isotope fractionation. The model results show that the evaporation rate from the treatment plots was higher than the control plots for both ecosystems. The water content, however, remained higher in the treatment plots because the control plots had additional soil water loss due to transpiration. The level of stable isotope enrichment does not depend only on total soil water loss. The greater level of stable isotope enrichment in the treatment plots is due to the fraction of soil water loss by evaporation being greater in the treatment plots than the control plots.

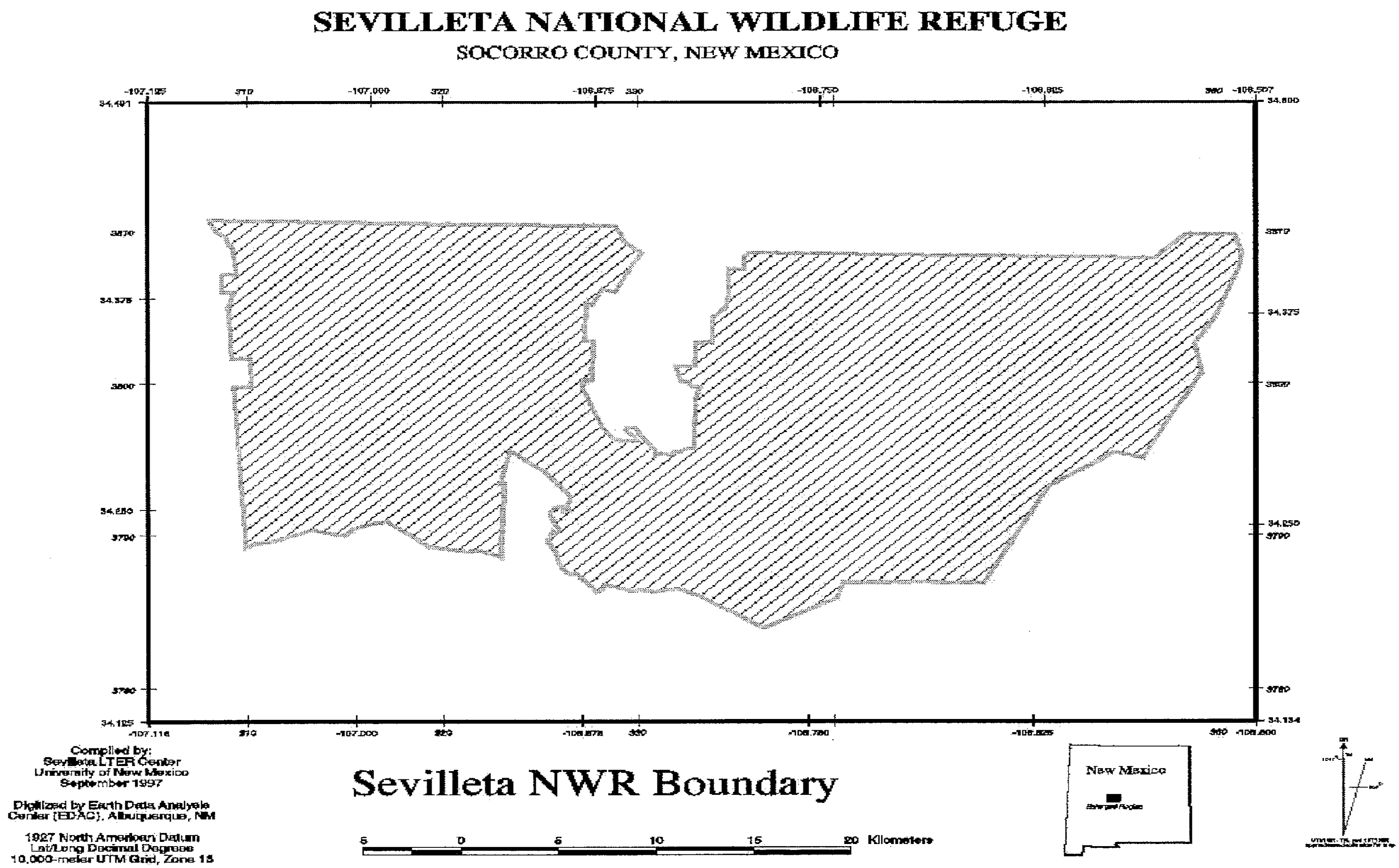

Figure 1.1: Location of the Sevilleta National Wildlife Refuge in central New Mexico.

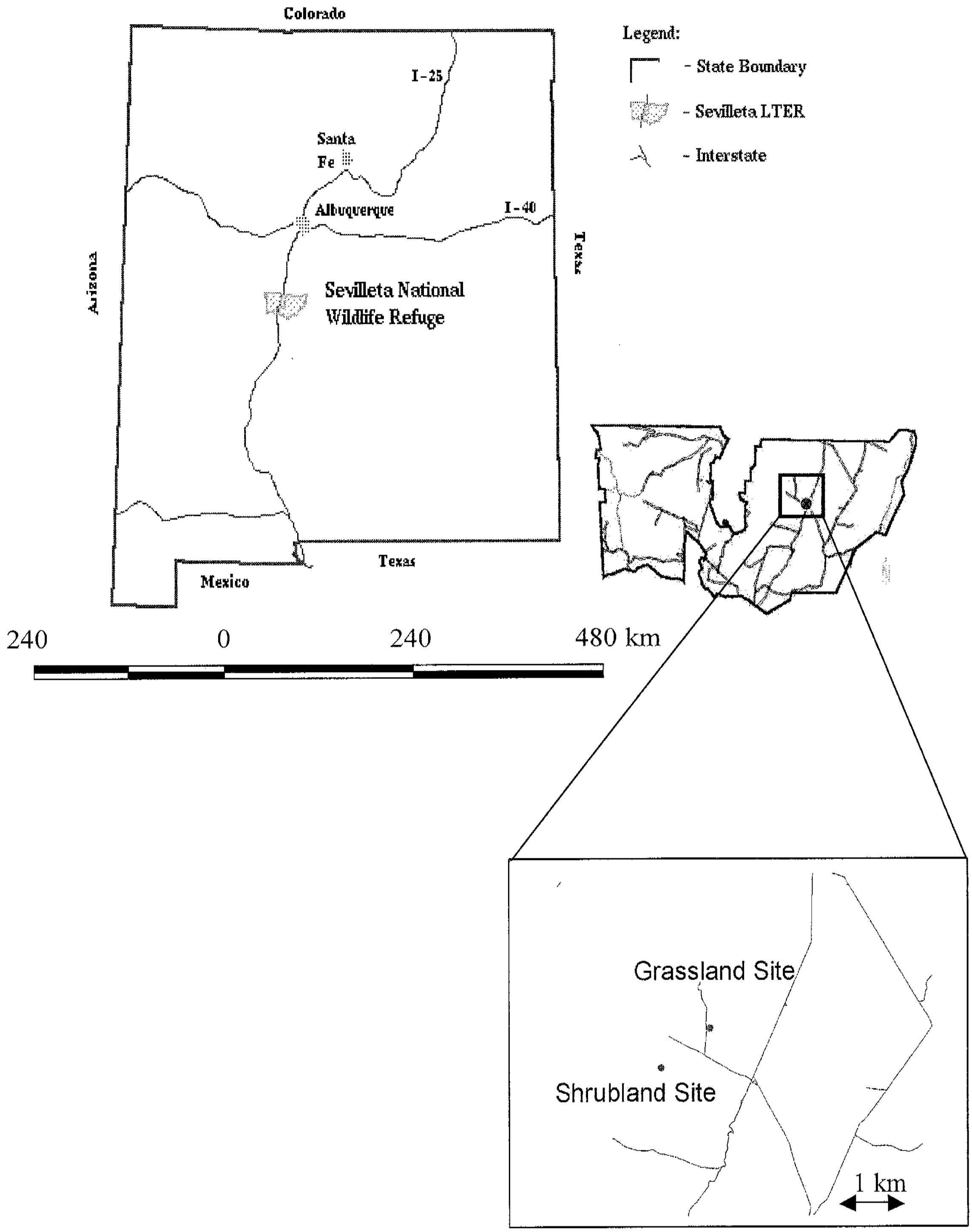

Figure 1.2: Approximate location of sampling sites for each ecosystem in the SNWR. Based on a WGS84 datum, the geographic coordinates for the grass ecosystem sampling sites are N34° 20.64' and W106° 43.63' at an elevation of 5268 feet above mean sea level (fmsl). The geographic coordinates for the shrub ecosystem sampling sites are N34° 20.41' and W106° 44.63' at an elevation of 5257 fmsl.

2. STABLE ISOTOPE CHEMISTRY

We apply the science of stable isotope geochemistry to the analysis of soil water. In order to outline the field and laboratory methods as well as develop a numerical stable isotope balance model, the fundamentals of stable isotope geochemistry are presented.

2.1 Stable-Isotope Conventions

Oxygen has three stable isotopes (^{16}O, ^{17}O, ^{18}O) and hydrogen has two stable isotopes (^{1}H, ^{2}H). The dominance of stable isotopes ^{16}O and ^{1}H (**Table 2.1**) in the water molecule make measuring absolute stable isotope abundances of the less common isotope in a sample quite difficult.

Element	Isotope	Atomic mass (amu)	Abundance (atom %)
Hydrogen	1H	1.007825	99.985
	2H (D or deuterium)	2.014102	0.015
Oxygen	16O	15.994915	99.76
	17O	16.999131	0.04
	18O	17.99916	0.2

Table 2.1: Summary of the stable H and O isotopes statistics **(Walker et al, 1989)**; 'amu' indicates 'atomic mass unit', the standard unit of mass for atoms and molecules.

Instead, absolute stable isotope abundances are measured as a ratio, R, shown in **Equation 2.1**.

$$R = (\text{\# of moles of less common isotope / \# of moles of more common isotope}) \quad \textbf{(2.1)}$$

For this study, $R(^2H) = {}^2H / {}^1H$ and $R(^{18}O) = {}^{18}O / {}^{16}O$. ^{18}O is used instead of ^{17}O because of the greater abundance and mass difference compared to ^{16}O, thus variations in $R(^{18}O)$ are more readily detectable than $R(^{17}O)$. Most studies evaluate stable isotopes of $R(^2H)$ and $R(^{18}O)$ relative to an international standard, V-SMOW. This study reports all stable-isotope data relative to V-SMOW. **Equation 2.2** illustrates how R-values, in this example $R(^2H)$, are measured and reported relative to V-SMOW:

$$\delta^2H(^0/_{00}) = \left(\frac{R(^2H)_{sample}}{R(^2H)_{V-SMOW}} - 1 \right) * 10^3 \qquad \textbf{(2.2)}$$

The multiplication by 10^3 allows for easy interpretation of measured values. According to convention, a value of 3.6 $^0/_{00}$ is easier to handle than an absolute value of 0.0036.

2.2 Meteoric Water Line

The Meteoric Water Line (MWL) is an empirical representation of meteoric waters (including most groundwater bodies) found throughout the world with respect to δ^2H and $\delta^{18}O$ **(Craig, 1961)**. The MWL summarizes the composition of precipitation worldwide. It provides the means for measuring $\delta^{18}O$ and δ^2H values against typical ranges found in nature. The typical range of $\delta^{18}O$ values for water involved in ecosystem processes generally is –30 and +40 $^0/_{00}$ **(Hayes, 1983)**. **Figure 2.1** illustrates the MWL with the empirical relationship shown in **Equation 2.3**:

$$\delta^2H = 8 * \delta^{18}O + 10 \qquad \textbf{(2.3)}$$

Of importance to this study, evaporation trends associated with low humidity environments develop slopes as low as 2 **(Campbell et al., 1995)**. In a high humidity environment, evaporation causes a slope similar to that of the MWL **(Chapman et al., 1992)**.

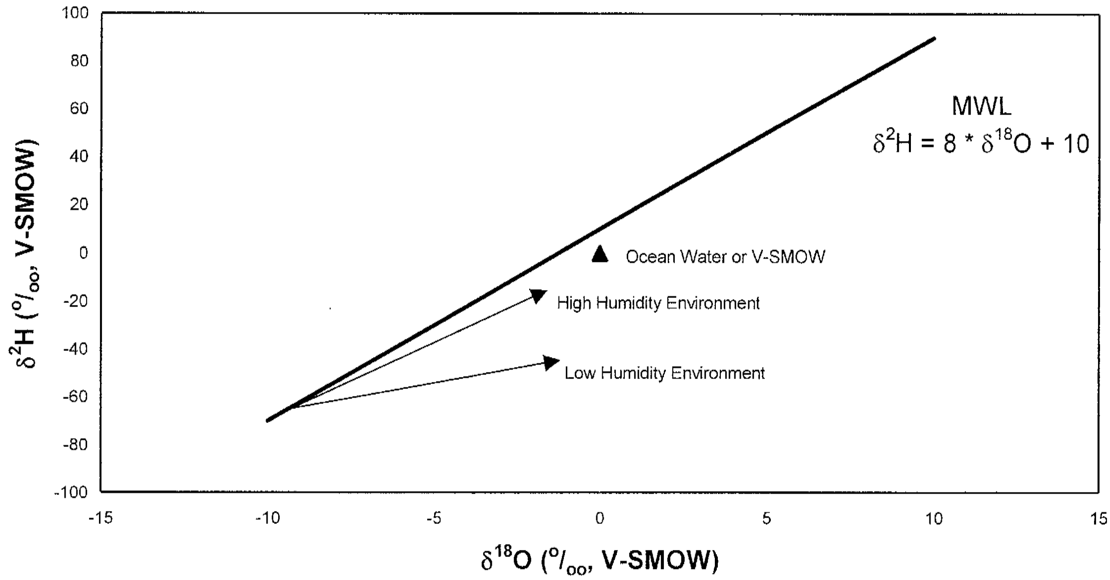

Figure 2.1: Meteoric Water Line based on **Craig (1961)**; modified from **Campbell and Larson (1998)**.

2.3 Stable Isotopes of Soil Water

Fractionation describes how stable isotopes of an element will partition into different phases. The stable isotopes of ^{2}H and ^{18}O will preferentially reside in liquid soil water since liquid water exhibits stronger hydrogen bonding than water vapor. Different processes will cause different degrees of fractionation of the same type of stable isotope. The theory and development of all relations for the phenomenon of fractionation will be discussed briefly. Readers wishing to gain a more substantial understanding are referred to **Criss (1999)** and **Campbell and Larson (1998)** and the many original sources referenced within them.

Isotopic fractionation between liquid water and water vapor can be ascribed by means of a fractionation factor, α_{LV}. α_{LV} represents the partitioning of isotopes between two separate phases. **Equation 2.4 and Equation 2.5** show how the equilibrium fractionation factor, α_{LV}, the measure of partitioning, depends on temperature and can be calculated based upon equations from **Majoube (1971)** for temperatures between 0 and 100°C:

$$10^3 * \ln \alpha_{LV} = 1.137E6 * T^{-2} - 415.6 * T^{-1} - 2.0667 \qquad \text{for } \delta^{18}O \qquad \textbf{(2.4)}$$

$$10^3 * \ln \alpha_{LV} = 24.844E6 * T^{-2} - 76{,}248 * T^{-1} + 52.612 \qquad \text{for } \delta^{2}H \qquad \textbf{(2.5)}$$

USGS professional paper 440-KK (**Friedman and O'Neil, 1977**) provides an alternate source for α in graphical format.

Evaporation of soil water will affect the fractionation of oxygen stable isotopes more than hydrogen stable isotopes based on diffusion and kinetic theory. **Equation 2.6** shows the fundamental equation available for computing kinetic energy (E_k)

$$E_k = \tfrac{1}{2}\, m\, v^2 \qquad \textbf{(2.6)}$$

where m represents the mass of a molecule and v represents that molecule's velocity. The two water molecules, $H_2{}^{16}O$ and $H_2{}^{18}O$, obviously have different mass (**Table 2.1**), yet at the same temperature, each water molecule possesses the same kinetic energy. As a result, the two different water molecules develop different velocities; $H_2{}^{16}O$ has a higher velocity than $H_2{}^{18}O$. During evaporation, the heavier molecule travels a shorter distance than the lighter molecule during the same interval of time and the residual liquid water in a soil become enriched relative to the initial value. In addition, the distance traveled in a soil (porous medium) is significantly greater than a typical open water body given the nature of the more tortuous pathways in soils. This serves to enhance the degree of enrichment and affects ^{18}O more than ^{2}H since ^{18}O has a larger mass difference from ^{16}O than ^{2}H has from ^{1}H.

Referring back to the meteoric water line in **Chapter 2.2: 'Meteoric Water Line'**, this effect develops slopes as a low as 2. Kinetic effects on the fractionation (kinetic fractionation) of H and O stable isotopes in soil water become more pronounced than the effects of equilibrium fractionation during evaporation. In **Equation 2.7**, a kinetic fractionation factor has been defined **(Shurbaji, 1994)** in an effort to better account for fractionation beyond those effects of equilibrium fractionation alone:

$$\sigma_i^{v} = \frac{D^{v*}}{D_i^{v*}} \qquad \textbf{(2.7)}$$

D^{v*} represents the water vapor diffusion coefficient and $D^{v*}{}_i$ represents the effective vapor diffusion coefficient of the isotope species of interest (eg. length^2/time).

As latent heat energy, available for evaporation and transpiration, interacts with soil and soil water, the vibrational energy associated with hydrogen bonding between liquid water molecules dictates the degree of stable isotope transport into the vapor phase **(Urey, 1947)**. A stable isotope of a particular element with a heavier atomic mass will preferentially reside in the phase exhibiting stronger bonding than a stable isotope of that same element with a lighter mass. It is this observation that allows the opportunity to exploit H and O stable isotopes as tracers of evaporation and transpiration in water balance studies.

3. FIELD METHODS

This chapter outlines the field methods for soil sample collection.

3.1 Sevilleta National Wildlife Refuge (SNWR)

The SNWR spans the middle Rio Grande Basin in Socorro County, New Mexico from the Los Pinos Mountains (2,195m) in the east to the foothills of Ladrone Peak (2797m) in the west (http://sevilleta.unm.edu). The field-sampling sites, situated east of the Rio Grande along the fringe of the northernmost extent of the Chihuahuan desert, were on an elevated plateau with a topographic slope less than a 2^{o} along a shrub-grass ecotone. The principal species include *Larrea tridentata* or creosotebush ('shrub') and *Bouteloua eriopoda* or black-grama grass ('grass').

The soil is classified mainly as sandy loam, although minor textural differences between the grass and shrub ecosystems have been documented **(Kieft et al., 1998)**. **Figure 3.1** shows the root density for the shrub and grass ecosystems in the SNWR as a function of depth. Soil and root samples were collected at 5 cm intervals below the plant (canopy) and below the intercanopy space for the root density study. The grasses' roots exist mainly in the upper 10 cm of soil while the shrubs' roots exist primarily in the 10-30 cm soil depth interval. In both ecosystems, a higher density of roots exists below the canopy than in the intercanopy spaces.

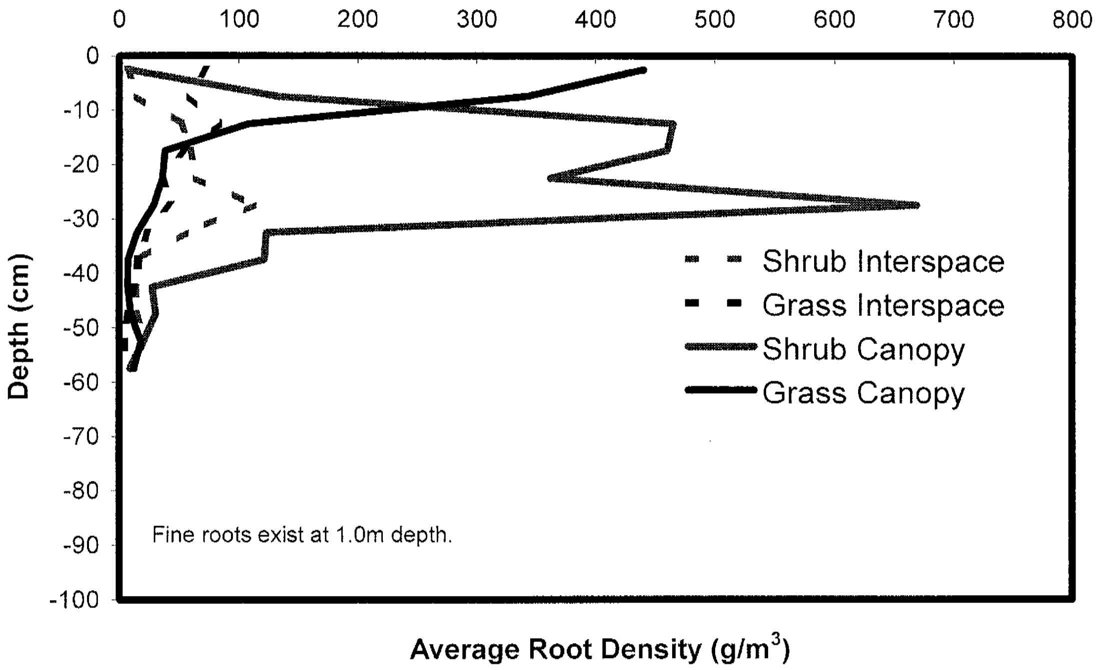

Figure 3.1: Root density as a function of depth for the shrub and grass ecosystems. Root density study conducted during Fall 2001. Density values (g/cm^3) reflect dry mass of roots per volume of soil collected.

3.2 Precipitation Event Monitoring and Precipitation Sample Collection

Several meteorological stations are situated throughout the SNWR that record precipitation among many other variables. The SNWR website (**http://sevilleta.unm.edu**) updates all records of precipitation on an hourly basis. After the wet-season began on approximately Julian Day 195±10 of the year 2002 (**Figure 3.2**), the normally dormant grasses began actively transpiring as evidenced by the sprouting of new leaves.

In order to partition ET into evaporation and transpiration with a mass-balance approach using stable-isotope geochemistry as a tool, we need to collect a sample of the precipitation event water. The event on Julian Day 214-215 was selected. The stable isotope signature of the precipitation is needed as a check on the initial soil water stable isotope signature, as it will likely change from the original value before the event to after the event. Following the precipitation collection system design of **Friedman et al. (1992)**, we constructed our own precipitation collection system (**Figure 3.3**).

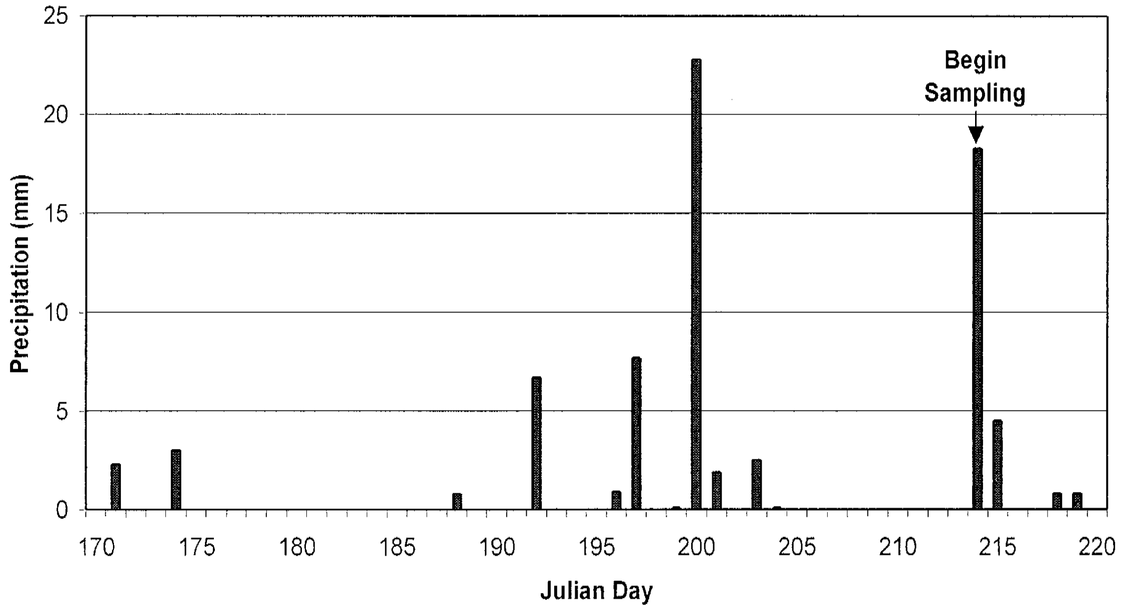

Figure 3.2: Precipitation records from SNWR Five Points meteorological station for Julian Days 170-220 of the year 2002. The precipitation event of focus for our study occurred in the late evening of Julian Day 214 into the early morning hours of Julian Day 215.

Precipitation settles below the mineral oil layer in the glass collection jar since the ρ_{water} (1.0g/mL) is greater than $\rho_{mineral\ oil}$ (~0.84g/mL). Mineral oil does not evaporate on the time-scale of interest during this study and prevents the evaporation of any captured precipitation. The system was tested between April 12th and July 3rd, 2002 and recorded ~14mm equivalent depth of precipitation. The SNWR Five Points rain gauge, located <0.5km from the test system, recorded 13.7mm equivalent depth of precipitation.

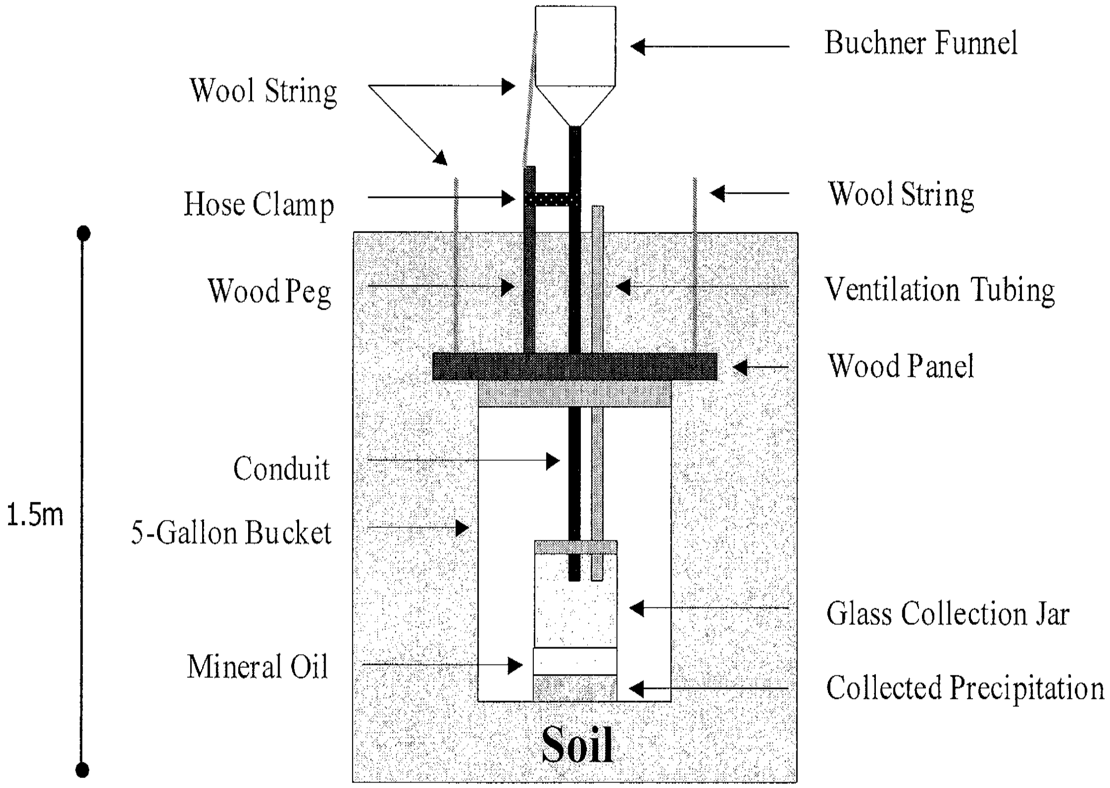

Figure 3.3: Precipitation collection system design modified from **Friedman et al., 1992**. This figure is not to scale.

3.3 Control vs. Treatment

One common design for an experiment is to deliberately impose a treatment onto a group of randomly selected individuals in order to observe the response. The response is then compared to a group of individuals whom did not experience any treatment (control). The treatment in this study was the elimination of transpiration while the individuals were the two plant types, shrub and grass.

The control and treatment plots were randomly selected to remove bias and capture the natural heterogeneity in each ecosystem. We performed the random sampling by means of a uniform grid with plots of representative size that were selected by a random number generator **(Thompson, 1992)**. Twenty-five plots comprised the grass ecosystem grid encompassing a total area of $625m^2$ (25m x 25m) while twenty-five plots comprised the shrub ecosystem grid encompassing an area of 2500 m^2 (50m x 50m). We assigned each plot within each grid a number from 1 to 25 beginning in the northwest corner and moving to the right by column (**Figure 3.4**). The 'randperm' function in MATLAB®6 generates uniformly distributed random numbers within a prescribed interval and selects each number only once. The first plot selected for each ecosystem became the control plot and the second became the treatment plot.

We did not remove the plants from each treatment plot in order to maintain consistent ecosystem dynamics in terms of interception and infiltration patterns during the precipitation event and shading during the post-precipitation drying period. **Table 3.1** summarizes our findings of the most suitable herbicide that stopped the transpiration by grasses as indicated by a change from a green to a tan color yet retained the overall grass structure. Spectracide was used for the grass treatment.

For the shrub ecosystem, transpiration was stopped by physical not chemical means. The shrub treatment involved cutting the main shrub branches from the basal stem and harnessing the cut-off branches back onto the basal stem with wool string. Several tests were performed to evaluate whether or not creosote bush would maintain its structure once the branches were cut. Creosote bush is remarkably resistant to wilting for up to two weeks after cutting the branches. The precipitation event of focus in this study occurred on the second evening after the cutting. Not only would the general interception and infiltration patterns observed by **Bhark (2002)** and **Bhark and Small (2003)** be maintained during the event, but the shrub shading pattern would still affect the post-precipitation drying. **Figure 3.5** provides a cartoon illustrating the shrub treatment.

Grass Site Grid: Grid Size = 25 m x 25 m ($625m^2$); Plot Size = 5m x 5m

1	2	3	4	5
6	7	8	9	10
11	12	13	14	15
16	17	18	19	20
21	22	23	24	25

	Randomly Generated Number
Treatment	15
Control	12

Shrub Site Grid: Grid Size = 50m x 50m ($2500m^2$); Plot Size = 10m x 10m

1	2	3	4	5
6	7	8	9	10
11	12	13	14	15
16	17	18	19	20
21	22	23	24	25

	Randomly Generated Number
Treatment	21
Control	19

Figure 3.4: Twenty-five plot grids for each ecosystem from which control and treatment plots were randomly selected by the MATLAB® 6 'randperm' function.

Pesticide	Active Ingredient	Vegetation Killed?	Structure Retention?
Spectracide	diquat dibromide	Yes	Yes
Enforce 'Roots & All'	glyphosphate	No	Yes
Finale	glufosinate-ammonium	Yes	No

Table 3.1: Summary of common herbicides and findings associated with the elimination of transpiration and structure retention.

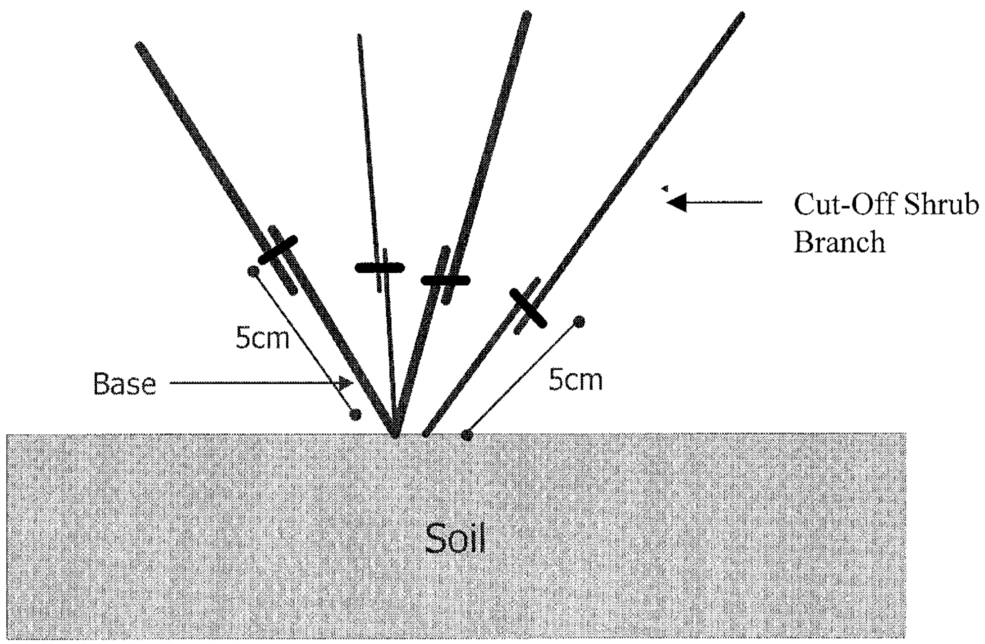

Figure 3.5: Cartoon illustration of the shrub treatment. All cuts were made approximately 5 cm from the ground surface. The overall structure of the shrubs was maintained for up to two weeks after cutting (~1 ½ weeks after the precipitation event). This figure is not to scale.

3.4 Soil Sampling

Soil samples were collected before, immediately after and for 6 consecutive days following the fourth precipitation event, Julian Day 214-215 (**Figure 3.2**). All canopy and intercanopy space localities in each plot, as listed below, were given a number starting from one to the total number of each soil locality per plot. The MATLAB®6 'randperm' function selected three localities for sampling per plot per ecosystem per sampling day. On each sampling day, we collected the soil samples of a specified volume (**Figure 3.6**) from the randomly selected localities over the 0-10cm and 10-30cm soil depth interval. The localities are listed as follows:

- Shrub ecosystem, control plot, canopy soil
- Shrub ecosystem, control plot, intercanopy space
- Shrub ecosystem, treatment plot, canopy soil
- Shrub ecosystem, treatment plot, intercanopy space
- Grass ecosystem, control plot, canopy soil
- Grass ecosystem, control plot, intercanopy space
- Grass ecosystem, treatment plot, canopy soil
- Grass ecosystem, treatment plot, intercanopy space

Volumetric water content (**Equation 3.1**) can be calculated if the soil sample volume is known and the volume of water in the soil sample is estimated.

$$\theta_V = V_w / V_{soil} \qquad \textbf{(3.1)}$$

V_w represents volume of water in the soil sample and V_{soil} represents the volume of the soil matrix, water and air. θ_v (volumetric water content) is a dimensionless quantity. The volume of water in each soil sample was determined using cryogenic vacuum distillation techniques (**Chapter 4.1: Cryogenic Vacuum Distillation**). After each sample of soil was collected, it was placed into its own mason jar to prevent any loss of water. All samples were transported in a cooler to the laboratory.

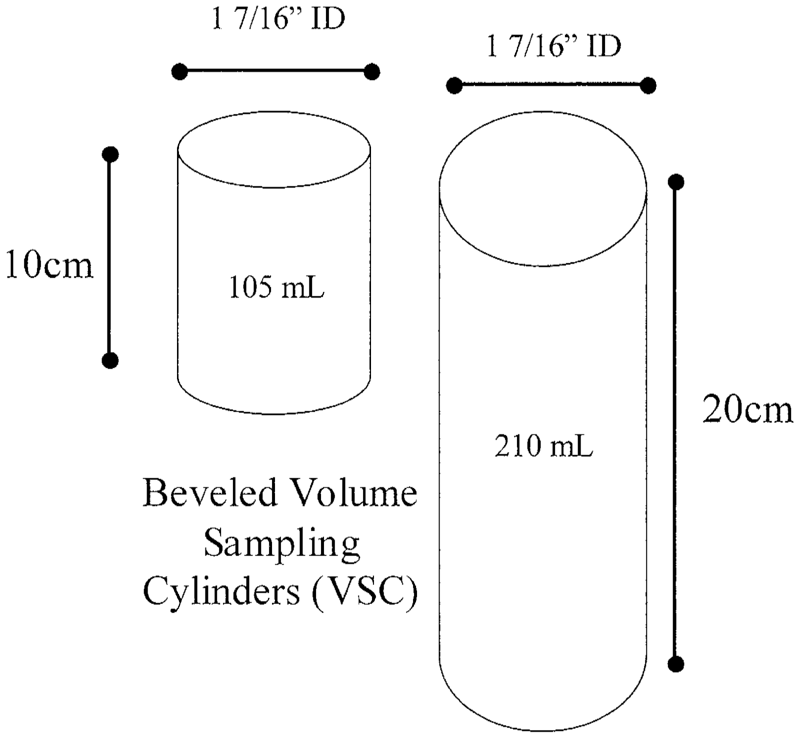

Figure 3.6: Dimensions of the soil sampling cylinders used in this study. The cylinders were beveled for easier penetration into the soil. This figure is not to scale.

4. STABLE ISOTOPE LABORATORY METHODS

This chapter summarizes the methods involved with the extraction of soil water from the soil sample (cryogenic vacuum distillation), the equilibration of CO_2 with soil water for $\delta^{18}O$ analysis, and Zn reduction for $\delta^{2}H$ analysis of soil water. All stable isotope analyses were performed on a Finnigan MAT Delta E isotope ratio mass spectrometer using Oztech gas standards in the Stable Isotope Mass Spectrometry Laboratory, operated by Dr. Andrew Campbell, at New Mexico Institute of Mining & Technology (N.M.I.M.T.).

4.1 Cryogenic Vacuum Distillation

Cryogenic vacuum distillation is a method for removing the soil water from the soil sample without overall stable isotope fractionation. The first step involves pre-weighing the 1000mL glass flask that houses the soil sample for the duration of the soil water extraction. The soil sample is introduced into the 1000mL flask, quickly isolated from atmosphere, and placed in liquid nitrogen (-180°C). Once all soil water is frozen (~30 minutes of freezing), the glass apparatus is pumped to vacuum. Vacuum reduces the contamination from atmospheric water vapor and helps extract soil water during the heating step. After vacuum is achieved, the glass apparatus containing the soil and frozen soil water is placed onto an electric heater. For two to three hours the electric heater drives water vapor into a separate, 100mL glass flask that rests in a liquid nitrogen dewar. Once all of the soil water is extracted, the 100mL flask containing the collected soil water is removed from the dewar and the soil water is placed into vials with polyseal lids to further prevent atmosphere contamination. The mass of water can be determined if the vials are pre-weighed.

4.2 $\delta^{18}O$ Analysis via CO_2-H_2O Equilibration

Socki et al. (1992) described an extraction technique for the determination of $\delta^{18}O$ in water using pre-evacuated glass vials. The method used at N.M.I.M.T. is calibrated for 0.5mL of water per analysis. First, CO_2 of known isotopic composition is loaded into the pre-evacuated vials on the extraction line. Then, 0.5mL of the soil water is injected through the septum on the vial top with a disposable syringe. The vials are then placed into a heated shaker bath (300 cps) for a minimum of four hours to accelerate the equilibration process. The laboratory uses the $CO_2(g)$-$H^2O(l)$ equation from **Bottinga (1968)** to calculate the initial $\delta^{18}O$ of the water. The initial $\delta^{18}O$ of the water can be computed from **Equation 4.1**and **4.2** taken from **Campbell and Larson, 1998**:

$$\delta^{18}O^{i}_{H2O} = \frac{Y}{X}(\delta^{18}O^{f}_{CO2} - \delta^{18}O^{i}_{CO2}) + \delta^{18}O^{f}_{CO2} + \Delta_{CO2-H2O} \qquad \textbf{(4.1)}$$

where

$$\Delta_{CO2-H2O} = \delta^{18}O_{CO2} - \delta^{18}O_{H2O} \qquad \textbf{(4.2)}$$

represents relative isotopic fractionation (or enrichment factor), which depends on the temperature of equilibration. Y and X are the amount of the two phases involved in the equilibration procedure. The mass spectrometer measures the $\delta^{18}O^{f}_{CO2}$ (final stable isotope composition of the carbon dioxide) while the $\delta^{18}O^{i}_{CO2}$ (initial stable isotope composition of the carbon dioxide) is known. The precision of this method is 0.1 $^{o}/_{oo}$.

4.3 δ^2H Analysis via Zn Reduction

The Zn reduction method **(Coleman et al., 1982; Kendall and Coplen, 1985)** was employed to produce hydrogen gas, H_2, from the soil water samples which was introduced to the mass spectrometer for δ^2H determination. The Zn reduction method requires 3μL of water per analysis. Such a small volume of water can be isolated through a glass capillary. The entire capillary is then placed into a reaction vessel containing the Zn and frozen via liquid nitrogen. Once frozen, the vessel is evacuated then heated at 450°C for 30 minutes. Four water standards are run to calibrate this extraction technique. The precision of this method is ~1 $^{o}/_{oo}$.

5. SOIL WATER DATA

This chapter contains the $\delta^{18}O$ and $\delta^{2}H$ soil water data and volumetric water content (θ) data. The $\delta^{18}O$ and $\delta^{2}H$ data are plotted as a linear regression relative to the MWL for the sampling day before the precipitation event and for the sampling day six days after the precipitation event. The ANOVA (ANalysis Of VAriance) statistics for $\delta^{18}O$ control and treatment plot data in both ecosystems are also presented in this chapter. The θ data are presented including normalization procedures.

5.1 $\delta^{18}O$ and $\delta^{2}H$ Data

Certain soil samples were selected for analysis of soil water stable isotope composition. We analyzed soil water from soil samples collected on the day before the precipitation event (Day –X) and six days after the precipitation event (Day 6) for $\delta^{18}O$ and $\delta^{2}H$ data. Soil water from soil samples collected immediately after the precipitation event (Day 0) and two days after the precipitation event (Day 2) were analyzed for $\delta^{18}O$ data only. **Table 5.1** is a legend for **Table 5.2, 5.3** and **5.6**. For example, a soil sample collected in the grass ecosystem control plot from canopy soil for the 0-10cm soil depth interval will be referred to as 'GCC10'. **Table 5.2** summarizes the $\delta^{18}O$ soil water data from Day –X, Day 0, Day 2 and Day 6. **Table 5.3** summarizes the $\delta^{2}H$ soil water data from Day –X and Day 6. As mentioned in **Chapter 3.4: 'Soil Sampling'**, three replicate samples were taken from a soil sampling locality type per plot per ecosystem per day. The $\delta^{18}O$ and $\delta^{2}H$ data shown in **Table 5.2** and **Table 5.3** are the mean of the three replicate samples with the respective standard deviation.

CATEGORY	SYMBOL	DEFINITION
1. Ecosystem	G	Grass
	S	Shrub
2. Sampling Plot	C	Control
	T	Treatment
3. Surface Cover Type	C	Canopy
	B	Bare
4. Soil Interval	10	0-10cm
	30	10-30cm

Table 5.1: Sample name legend for **Table 5.2, 5.3,** and 5.6; **Figure 5.11** through **5.14**; and occasionally within the text.

Soil water $\delta^{18}O$ and $\delta^{2}H$ data are plotted relative to the MWL **(Craig, 1961)** in **Figure 5.1** (Day –X) and **Figure 5.2** (Day 6). The slope on Day –X is 2.1 with an R^2 = 0.89 while the slope on Day 6 is 2.3 with an R^2 = 0.71. The precipitation was captured by our precipitation collection system and analyzed for $\delta^{18}O$ and $\delta^{2}H$ data ($\delta^{18}O$ = -7.2 $^{o}/_{oo}$, $\delta^{2}H$ = -50$^{o}/_{oo}$). A linear regression through the Day 6 $\delta^{18}O$ and $\delta^{2}H$ soil water data can be extended and shown to converge reasonably well with the MWL at the reported precipitation event $\delta^{18}O$ and $\delta^{2}H$ values as shown in **Figure 5.2**.

Summary of Soil Water $\delta^{18}O$

Grass Ecosystem Control Plot			Grass Ecosystem Treatment Plot			Shrub Ecosystem Control Plot			Shrub Ecosystem Treatment Plot		
GCB10	*Mean*	*Standard Deviation*	**GTB10**	*Mean*	*Standard Deviation*	**SCB10**	*Mean*	*Standard Deviation*	**STB10**	*Mean*	*Standard Deviation*
Day -X	14.6	1.5	Day -X	14.6	1.5	Day -X	13.0	2.2	Day -X	13.0	2.2
Day 0	-2.8	2.5	Day 0	-4.4	3.5	Day 0	-5.1	1.7	Day 0	-3.2	1.6
Day 2	-1.1	2.4	Day 2	0.7	1.4	Day 2	-1.1	1.9	Day 2	0.9	2.3
Day 6	2.9	1.9	Day 6	3.5	2.3	Day 6	2.8	1.8	Day 6	1.3	0.5
GCC10	*Mean*	*Standard Deviation*	**GTC10**	*Mean*	*Standard Deviation*	**SCC10**	*Mean*	*Standard Deviation*	**STC10**	*Mean*	*Standard Deviation*
Day -X	2.0	1.0	Day -X	2.0	1.0	Day -X	4.3	0.4	Day -X	4.3	0.4
Day 0	-7.2	0.4	Day 0	-6.7	0.03	Day 0	-5.1	1.1	Day 0	-4.4	1.8
Day 2	-4.4	1.0	Day 2	-4.4	0.2	Day 2	-2.7	0.7	Day 2	-2.3	1.9
Day 6	-3.2	0.7	Day 6	-1.6	0.9	Day 6	-0.9	0.3	Day 6	1.3	0.6
GCB30	*Mean*	*Standard Deviation*	**GTB30**	*Mean*	*Standard Deviation*	**SCB30**	*Mean*	*Standard Deviation*	**STB30**	*Mean*	*Standard Deviation*
Day -X	11.1	0.7	Day -X	11.1	0.7	Day -X	8.9	1.5	Day -X	8.9	1.5
Day 0	3.8	4.4	Day 0	3.1	1.0	Day 0	1.8	2.8	Day 0	4.9	1.1
Day 2	0.7	3.5	Day 2	2.2	1.3	Day 2	4.1	5.9	Day 2	4.9	0.5
Day 6	5.5	2.3	Day 6	3.3	0.6	Day 6	5.4	1.8	Day 6	4.7	0.6
GCC30	*Mean*	*Standard Deviation*	**GTC30**	*Mean*	*Standard Deviation*	**SCC30**	*Mean*	*Standard Deviation*	**STC30**	*Mean*	*Standard Deviation*
Day -X	1.8	2.0	Day -X	1.8	2.0	Day -X	4.2	1.5	Day -X	4.2	1.5
Day 0	-6.1	1.7	Day 0	-4.3	1.6	Day 0	-1.3	3.7	Day 0	-0.2	1.3
Day 2	-4.3	0.9	Day 2	-5.0	0.1	Day 2	-0.1	0.2	Day 2	-0.8	2.5
Day 6	-3.6	0.4	Day 6	-3.0	0.4	Day 6	0.5	1.9	Day 6	0.2	1.0

Table 5.2: Summary of $\delta^{18}O$ soil water data from the sampling day soils selected for stable isotope composition analysis. $\delta^{18}O$ data represent the mean of 3 samples; standard deviations included.

Summary of Soil Water δ^2H

Grass Ecosystem Control Plot			Grass Ecosystem Treatment Plot			Shrub Ecosystem Control Plot			Shrub Ecosystem Treatment Plot		
GCB10	*Mean*	*Standard Deviation*	**GTB10**	*Mean*	*Standard Deviation*	**SCB10**	*Mean*	*Standard Deviation*	**STB10**	*Mean*	*Standard Deviation*
Day -X	-13.8	6.2	Day -X	-13.8	6.2	Day -X	-14.7	4.4	Day -X	-14.7	4.4
Day 6	-29.9	3.0	Day 6	-29.8	6.5	Day 6	-37.0	9.5	Day 6	-35.7	2.9
GCC10	*Mean*	*Standard Deviation*	**GTC10**	*Mean*	*Standard Deviation*	**SCC10**	*Mean*	*Standard Deviation*	**STC10**	*Mean*	*Standard Deviation*
Day -X	-45.1	3.5	Day -X	-45.1	3.5	Day -X	-32.5	0.9	Day -X	-32.5	0.9
Day 6	-47.6	5.1	Day 6	-42.2	2.8	Day 6	-43.3	4.3	Day 6	-31.1	2.6
GCB30	*Mean*	*Standard Deviation*	**GTB30**	*Mean*	*Standard Deviation*	**SCB30**	*Mean*	*Standard Deviation*	**STB30**	*Mean*	*Standard Deviation*
Day -X	-19.7	3.4	Day -X	-19.7	3.4	Day -X	-27.1	3.9	Day -X	-27.1	3.9
Day 6	-30.6	4.0	Day 6	-36.7	3.9	Day 6	-31.3	3.2	Day 6	-31.6	2.6
GCC30	*Mean*	*Standard Deviation*	**GTC30**	*Mean*	*Standard Deviation*	**SCC30**	*Mean*	*Standard Deviation*	**STC30**	*Mean*	*Standard Deviation*
Day -X	-36.8	7.0	Day -X	-36.8	7.0	Day -X	-29.7	1.5	Day -X	-29.7	1.5
Day 6	-53.0	4.1	Day 6	-48.4	1.9	Day 6	-38.7	3.3	Day 6	-38.5	4.9

Table 5.3: Summary of δ^2H soil water data from sampling day soils selected for stable isotope composition analysis. δ^2H data shown represent the mean of 3 samples; standard deviations included.

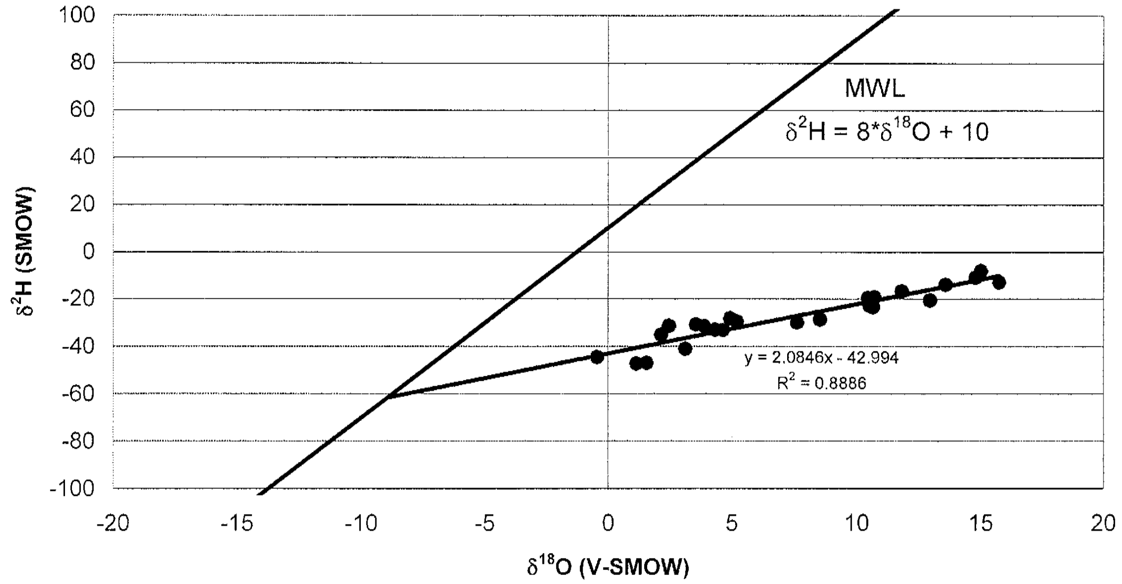

Figure 5.1: Soil water $\delta^{18}O$ and $\delta^{2}H$ data plotted relative to the MWL **(Craig, 1961)** from all Day –X soil samples.

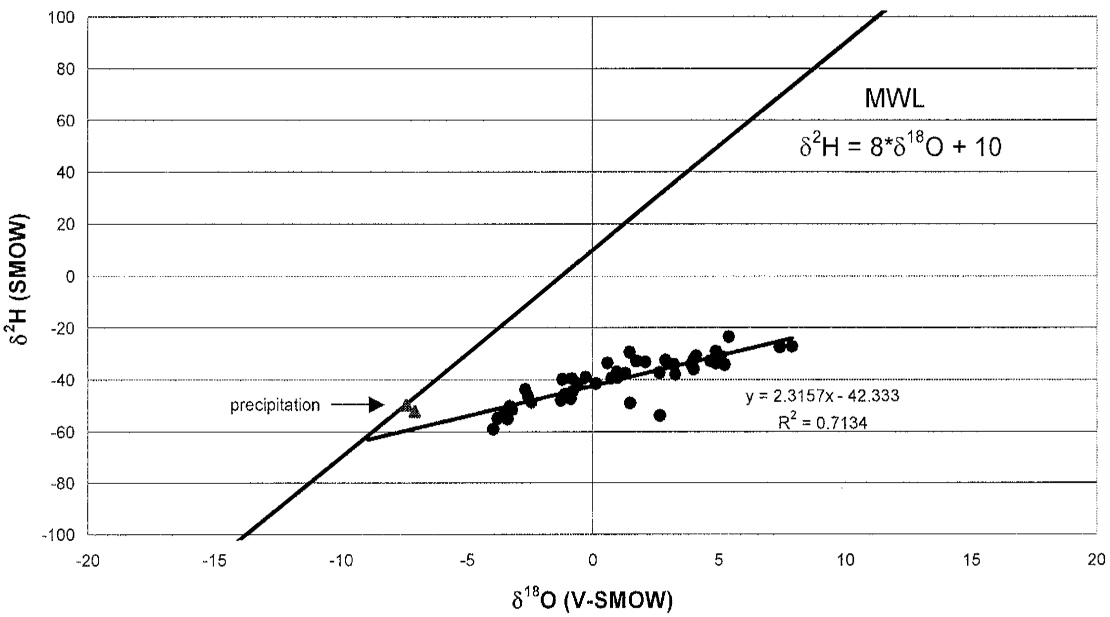

Figure 5.2: Soil water $\delta^{18}O$ and $\delta^{2}H$ data plotted relative to the MWL **(Craig, 1961)** from all Day 6 soil samples. The $\delta^{18}O$ and $\delta^{2}H$ data for the precipitation are shown on this figure and in **Figure 5.5** through **Figure 5.8**.

The slope on Day –X for the shrub ecosystem is 1.8 with an $R^2 = 0.88$ (**Figure 5.3**) while the slope on Day –X for the grass ecosystem is 2.2 with an $R^2 = 0.92$ (**Figure 5.4**). In both the shrub and grass ecosystems, the soil water from the intercanopy spaces are more enriched than the soil water from the canopy soils. No appreciable difference in the $\delta^{18}O$ and δ^2H soil water data is observed between the 0-10cm and 10-30cm canopy soil depth intervals. The 0-10cm intercanopy space soil water is slightly more enriched than the 10-30cm intercanopy space soil water in both ecosystems.

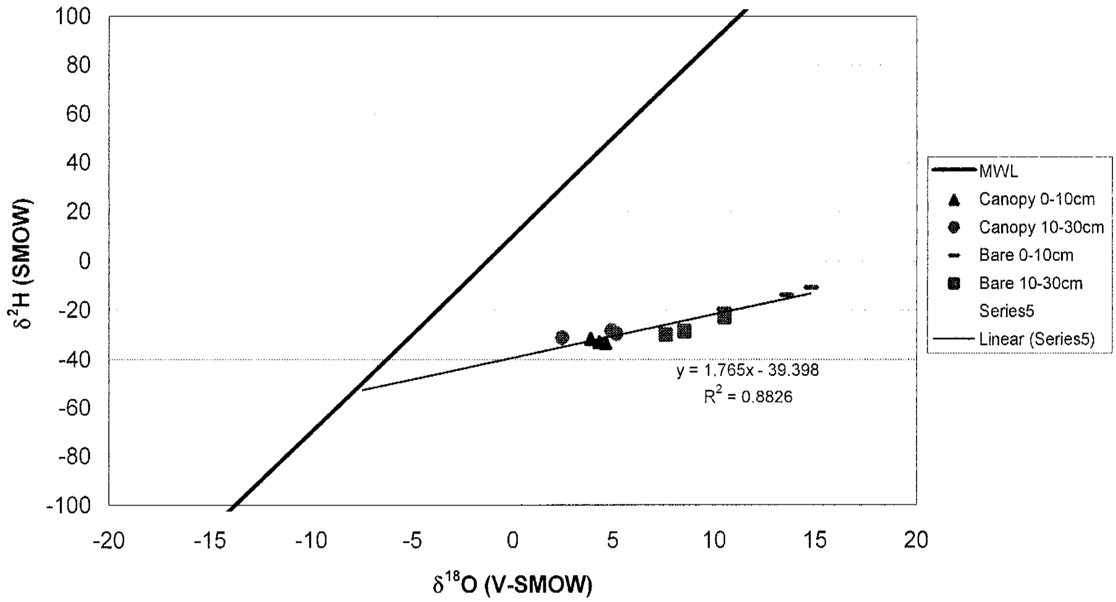

Figure 5.3: Shrub ecosystem 0-10cm and 10-30cm canopy and intercanopy space soil water $\delta^{18}O$ and δ^2H data plotted relative to the MWL **(Craig, 1961)** for Day -X.

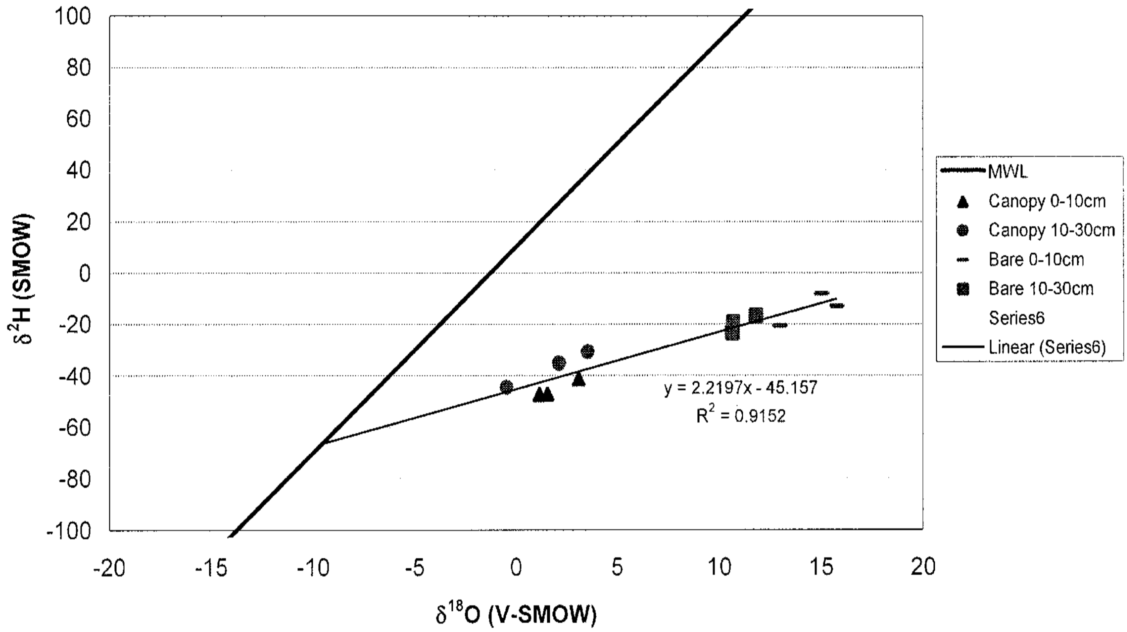

Figure 5.4: Grass ecosystem 0-10cm and 10-30cm canopy and intercanopy space soil water $\delta^{18}O$ and $\delta^{2}H$ data plotted relative to the MWL **(Craig, 1961)** for Day -X.

The slope on Day 6 for the shrub ecosystem control plot is 2.1 with an R^2 = 0.68 (**Figure 5.5**) while the slope on Day 6 for the shrub ecosystem treatment plot is 1.6 with an R^2 = 0.38 (**Figure 5.6**). The slope on Day 6 for the grass ecosystem control plot is 2.6 with an R^2 = 0.94 (**Figure 5.7**) while the slope on Day 6 for the grass ecosystem treatment plot is 2.0 with an R^2 = 0.52 (**Figure 5.8**). No appreciable difference is observed between any 0-10cm and 10-30cm soil water.

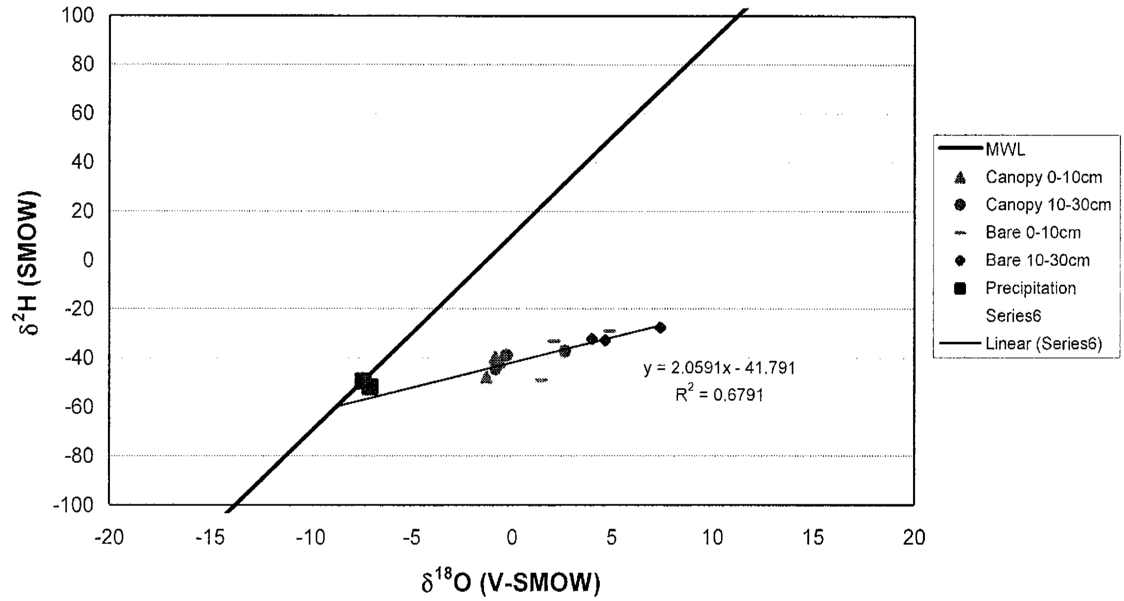

Figure 5.5: Shrub ecosystem control plot 0-10cm and 10-30cm canopy and intercanopy space soil water $\delta^{18}O$ and δ^2H data plotted relative to the MWL **(Craig, 1961)** for Day 6.

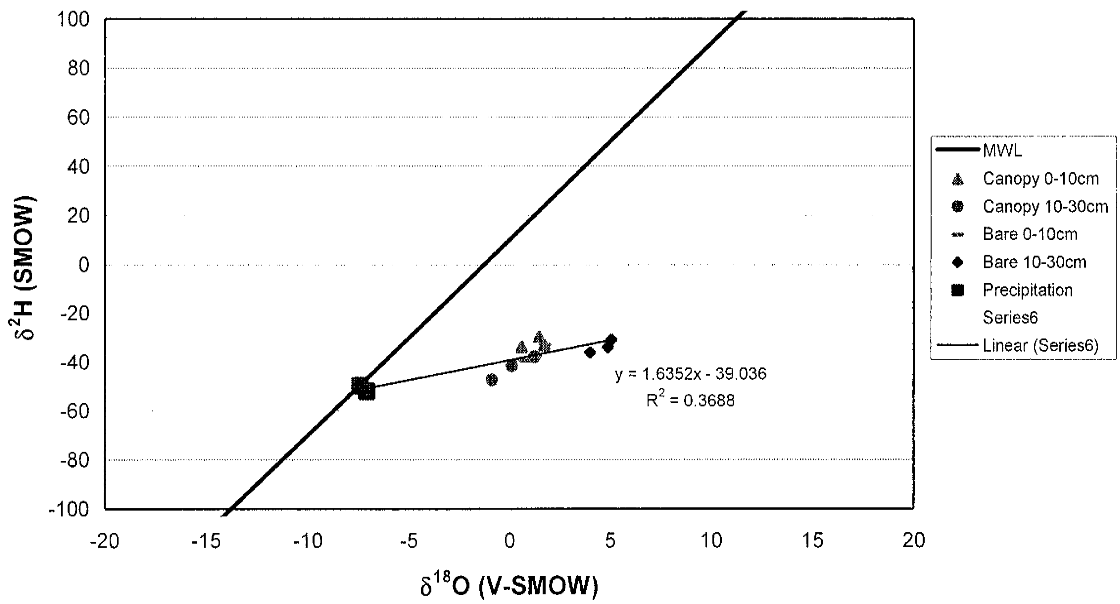

Figure 5.6: Shrub ecosystem treatment plot 0-10cm and 10-30cm canopy and intercanopy space soil water $\delta^{18}O$ and δ^2H data plotted relative to the MWL **(Craig, 1961)** for Day 6.

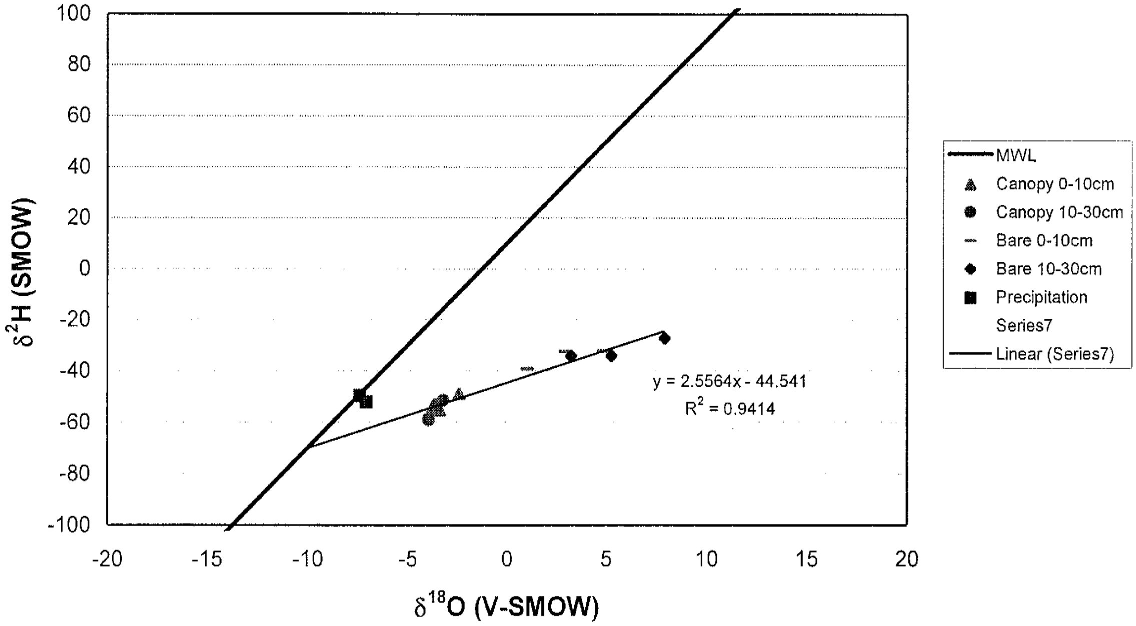

Figure 5.7: Grass ecosystem control plot 0-10cm and 10-30cm canopy and intercanopy space soil water $\delta^{18}O$ and $\delta^{2}H$ data plotted relative to the MWL **(Craig, 1961)** for Day 6.

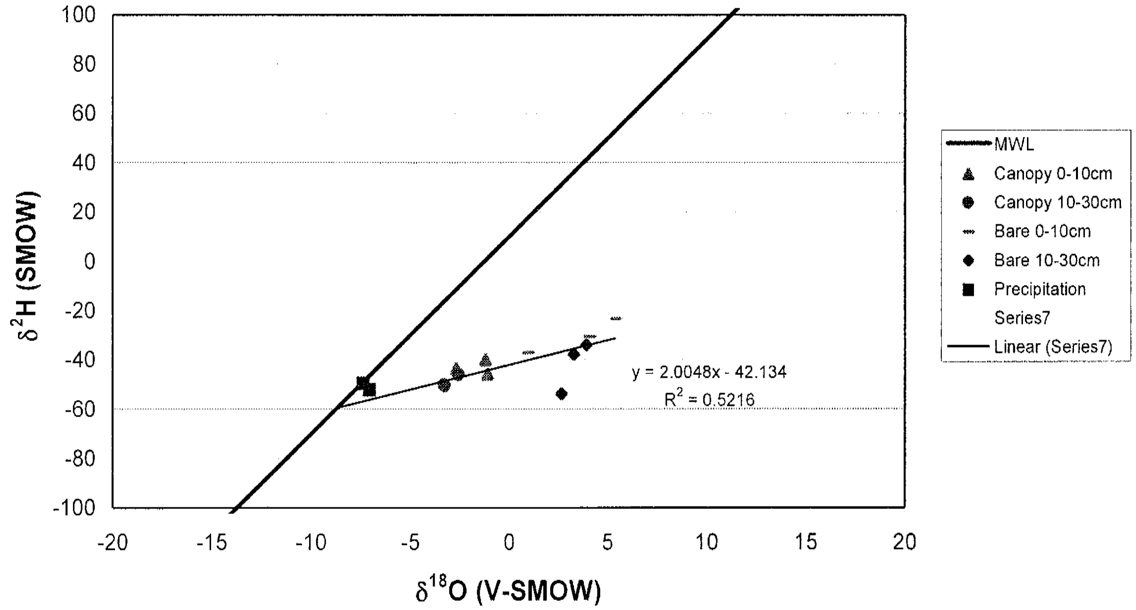

Figure 5.8: Grass ecosystem treatment plot 0-10cm and 10-30cm canopy and intercanopy space soil water $\delta^{18}O$ and $\delta^{2}H$ data plotted relative to the MWL **(Craig, 1961)** for Day 6.

5.2 Control vs. Treatment: $\delta^{18}O$

ANOVA, or ANalysis Of VAriance, provides a tool to determine if two datasets are statistically different. Readers wishing to gain a more substantial understanding are referred to **Moore and McCabe (2003)**. The following discussion includes the results from ANOVA tests for control and treatment plot soil water $\delta^{18}O$ data on Day 0, Day 2 and Day 6. The comparison between control and treatment plots will help detect if the process of transpiration causes any statistical significance between the soil water $\delta^{18}O$ datasets. Only $\delta^{18}O$ data was selected because $\delta^{2}H$ data was not available on Day 0 and Day 2, therefore ANOVA tests on Day 6 $\delta^{2}H$ data alone would not provide sufficient explanation for any trends observed with $\delta^{18}O$ data.

For this study, we specified a 90% confidence interval; this corresponds to a 0.10 critical value (α). The standard is a 95% confidence interval with a corresponding $\alpha = 0.05$. The confidence interval was decreased given the number of samples per dataset was three. A lower confidence level is appropriate because sample variability will more strongly affect a small sample population. In addition, the effects of transpiration on soil water $\delta^{18}O$ values are anticipated to be subtle. Each comparison on each day will yield its own P-value. Two-tail significance tests with unequal variances were done for each comparison. If the P-value falls below 0.10 then any observed difference in the soil water $\delta^{18}O$ data is statistically significant. If the P-value falls above 0.10 then any observed difference in the soil water $\delta^{18}O$ data is not statistically significant. **Table 5.4** summarizes the P-values from all ANOVA tests.

Summary of ANOVA Statistics: P-Values			
Grass Ecosystem		Shrub Ecosystem	
Surface Cover and Depth Interval	*Control vs. Treatment*	**Surface Cover and Depth Interval**	*Control vs. Treatment*
Bare 0-10cm		**Bare 0-10cm**	
Day 0	0.577	Day 0	0.238
Day 2	0.335	Day 2	0.332
Day 6	0.753	Day 6	0.273
Canopy 0-10cm		**Canopy 0-10cm**	
Day 0	0.145	Day 0	0.569
Day 2	0.953	Day 2	0.743
Day 6	0.08	Day 6	0.01
Bare 10-30cm		**Bare 10-30cm**	
Day 0	0.804	Day 0	0.178
Day 2	0.539	Day 2	0.842
Day 6	0.249	Day 6	0.576
Canopy 10-30cm		**Canopy 10-30cm**	
Day 0	0.262	Day 0	0.664
Day 2	0.289	Day 2	0.673
Day 6	0.195	Day 6	0.782

Table 5.4: Summary of ANOVA P-values given a 90% confidence interval and $\alpha = 0.10$ for the comparison of control and treatment plot soil water $\delta^{18}O$ data.

Figure 5.9 shows the 0-10cm shrub canopy soil water $\delta^{18}O$ data on Day 0, Day 2 and Day 6 for the comparison of control and treatment plots. **Figure 5.10** shows the 0-10cm grass canopy soil water $\delta^{18}O$ data on Day 0, Day 2 and Day 6 for the comparison of control and treatment plots. Based on **Figure 5.9** and **Figure 5.10**, the qualitative observation can be made that on Day 6 the 0-10cm canopy soil water for both ecosystems are different given the lack of overlapping standard deviation bars. The ANOVA statistics results shown in **Table 5.4** confirm this qualitative observation. Only the Day 6 0-10cm canopy soil water for both ecosystems yielded P-values less than 0.10.

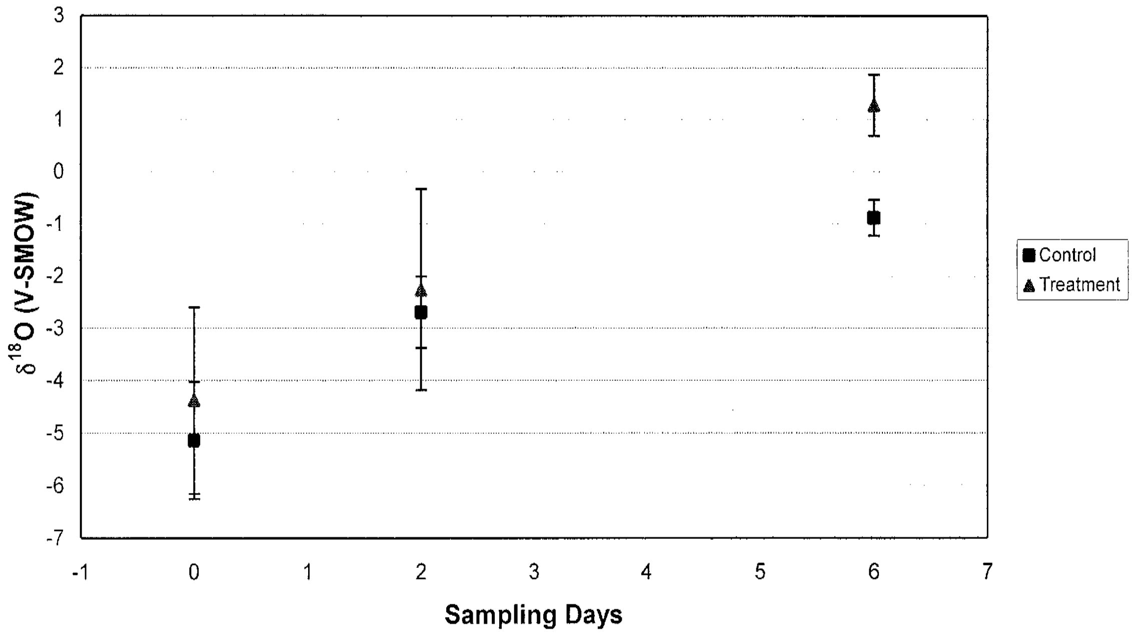

Figure 5.9: 0-10cm canopy soil water $\delta^{18}O$ data on Day 0, Day 2 and Day 6 for the comparison of control and treatment plots in the shrub ecosystem. ANOVA P-value = 0.01 on Day 6.

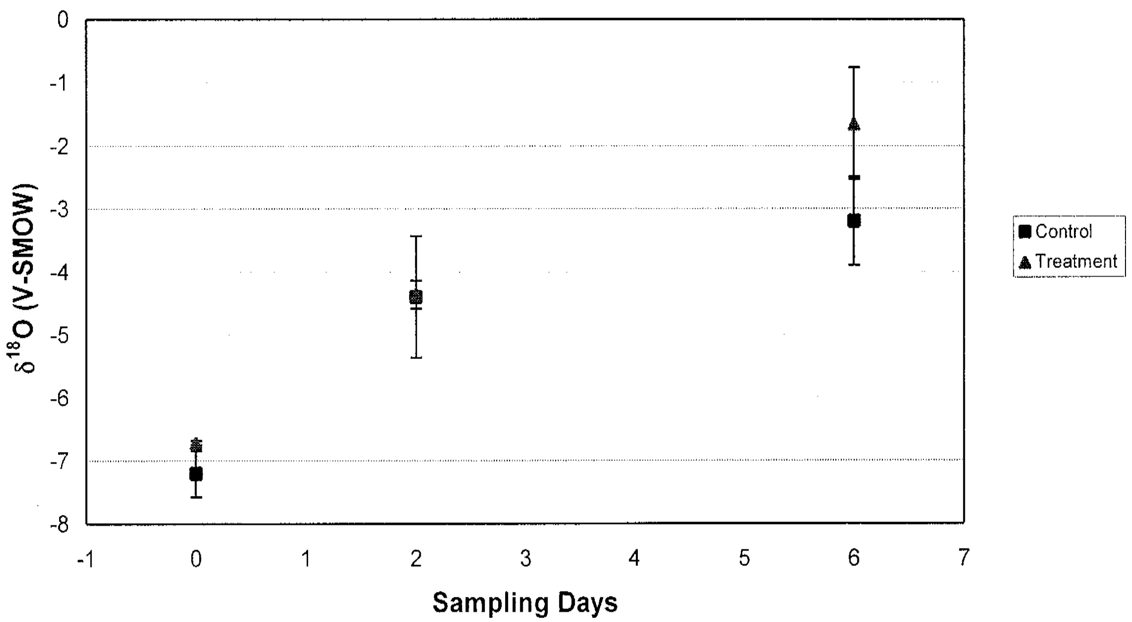

Figure 5.10: 0-10cm canopy soil water $\delta^{18}O$ data on Day 0, Day 2 and Day 6 for the comparison of control and treatment plots in the grass ecosystem. ANOVA P-value = 0.08 on Day 6.

5.3 Volumetric Water Content (θ) Data

The θ data is calculated from the cryogenic vacuum distillation results with dry bulk density (ρ_b) normalization. The cryogenic vacuum distillation methods provided soil water mass extracted per soil sample. We treat the soil water mass as equivalent to the soil water volume by assuming a density of water of 1.0 g/cm^3. As a check on the θ calculations (**Equation 3.1**), we estimated the ρ_b per soil sample to verify if the volume of soil sample was reasonably close to the anticipated value (**Figure 3.5**). It is unlikely that 50% of the ρ_b values for the soil samples were less than or equal to 1.0 g/cm^3 (the density of water). We believe the source of the uncertainty is from the presumed soil-sampling volume. As a consequence, we normalized the gravimetric water content (**Equation 5.1**) to θ as shown in **Equation 5.2** with dry bulk density values measured from members of our research group at N.M.I.M.T. under the guidance of Dr. Small.

$$\theta_g = \frac{M_w}{M_{soil}} \qquad \textbf{(5.1)}$$

θ_g represents the gravimetric water content, a dimensionless quantity. M_w represents the mass of water extracted from the soil sample from cryogenic vacuum distillation. M_{soil} represents the mass of the field soil.

$$\theta = \theta_g * \rho_b \qquad \textbf{(5.2)}$$

ρ_b represents the dry bulk density calculated as shown in **Equation 5.3**:

$$\rho_b = \frac{M_{soil}}{V_{soil}} \quad \textbf{(5.3)}$$

V_{soil} represents the anticipated volume of the soil sample from the volume soil sampling cylinders (**Figure 3.5**). However, the ρ_b values from **Table 5.5** were used in **Equation 5.1**. **Table 5.5** contains the dry bulk density values used for θ normalization for the 0-10cm soil depth interval.

Sampling Locality	Dry Bulk Density (g/cm^3)
Grass Canopy	1.170
Grass Bare	1.163
Shrub Canopy	1.211
Shrub Bare	1.200

Table 5.5: Dry bulk density values (g/cm^3) used for normalization of water content values for the 0-10cm soil depth interval. A value of 1.4 g/cm^3 was used for the 10-30cm soil depth interval based on group research under the guidance of Dr. Small at N.M.I.M.T.

Cryogenic vacuum distillation methods were only applied to Day –X, Day 0, Day 2 and Day 6 soil samples. We estimated the θ_g for the remaining soil samples from Day 1 and Day 3 through Day 5 using oven-dry methods and normalized the θ_g values to θ values using the ρ_b values from **Table 5.5** and **Equation 5.2**. Readers wishing to gain a description of the oven-dry method are referred to **Gardner (1986)**. **Table 5.6** contains the θ for all soil samples collected for this study (**Table 5.1** for the sample name legend). **Figure 5.11** through **Figure 5.14** show the normalized θ for the grass and shrub control and treatment plot soil samples over time.

Summary of Soil Volumetric Water Content

Grass Ecosystem Control Plot			Grass Ecosystem Treatment Plot			Shrub Ecosystem Control Plot			Shrub Ecosystem Treatment Plot		
GCB10	*Mean*	*Standard Deviation*	**GTB10**	*Mean*	*Standard Deviation*	**SCB10**	*Mean*	*Standard Deviation*	**STB10**	*Mean*	*Standard Deviation*
Day -X	4.1	0.7	Day -X	4.1	0.7	Day -X	5.7	0.6	Day -X	5.7	0.6
Day 0	16.1	1.7	Day 0	15.2	0.4	Day 0	13.9	2.6	Day 0	15.9	0.7
Day 1	12.5	1.3	Day 1	10.8	1.4	Day 1	8.4	1.3	Day 1	10.7	0.8
Day 2	10.4	0.9	Day 2	10.2	0.6	Day 2	11.4	0.5	Day 2	12.2	1.2
Day 3	9.2	1.5	Day 3	8.9	1.1	Day 3	8.2	0.1	Day 3	9.0	1.6
Day 4	10.0	2.0	Day 4	8.2	0.7	Day 4	7.1	0.3	Day 4	8.1	0.5
Day 5	8.2	1.1	Day 5	7.4	0.8	Day 5	6.9	0.8	Day 5	8.3	0.8
Day 6	8.4	1.1	Day 6	8.6	0.7	Day 6	7.0	0.4	Day 6	7.1	0.9
GCC10	*Mean*	*Standard Deviation*	**GTC10**	*Mean*	*Standard Deviation*	**SCC10**	*Mean*	*Standard Deviation*	**STC10**	*Mean*	*Standard Deviation*
Day -X	7.3	1.1	Day -X	7.3	1.1	Day -X	6.0	0.7	Day -X	6.0	0.7
Day 0	16.6	0.8	Day 0	16.5	0.8	Day 0	14.9	0.7	Day 0	16.2	0.4
Day 1	12.7	1.5	Day 1	11.0	0.7	Day 1	10.2	0.9	Day 1	9.5	0.4
Day 2	9.3	1.2	Day 2	9.8	0.7	Day 2	11.0	0.7	Day 2	10.6	1.1
Day 3	8.0	1.2	Day 3	7.3	0.3	Day 3	7.3	0.2	Day 3	7.6	0.3
Day 4	6.9	0.5	Day 4	8.4	0.7	Day 4	7.1	1.2	Day 4	6.9	1.3
Day 5	6.4	0.7	Day 5	6.9	1.7	Day 5	6.5	1.0	Day 5	7.3	1.2
Day 6	5.6	1.2	Day 6	9.2	2.2	Day 6	5.1	0.2	Day 6	7.7	0.3
GCB30	*Mean*	*Standard Deviation*	**GTB30**	*Mean*	*Standard Deviation*	**SCB30**	*Mean*	*Standard Deviation*	**STB30**	*Mean*	*Standard Deviation*
Day -X	5.5	0.8	Day -X	5.5	0.8	Day -X	6.8	0.4	Day -X	6.8	0.4
Day 0	15.9	1.6	Day 0	11.7	0.9	Day 0	14.4	1.8	Day 0	10.9	0.3
Day 1	15.1	2.4	Day 1	14.4	1.1	Day 1	9.2	1.3	Day 1	9.5	0.8
Day 2	16.9	2.5	Day 2	15.4	0.7	Day 2	10.3	1.4	Day 2	9.8	2.1
Day 3	12.9	2.4	Day 3	13.4	1.8	Day 3	9.7	2.0	Day 3	11.6	1.1
Day 4			Day 4			Day 4			Day 4		
Day 5	11.9	1.2	Day 5	13.0	0.3	Day 5	6.4	0.3	Day 5	8.8	0.7
Day 6	11.7	2.3	Day 6	12.5	0.9	Day 6	9.1	0.6	Day 6	10.4	0.2
GCC30	*Mean*	*Standard Deviation*	**GTC30**	*Mean*	*Standard Deviation*	**SCC30**	*Mean*	*Standard Deviation*	**STC30**	*Mean*	*Standard Deviation*
Day -X	9.8	0.5	Day -X	9.8	0.5	Day -X	9.7	0.9	Day -X	9.7	0.9
Day 0	25.6	1.4	Day 0	18.7	0.7	Day 0	14.7	3.8	Day 0	13.0	1.3
Day 1	17.8	1.1	Day 1	15.1	1.5	Day 1	12.1	1.2	Day 1	12.3	2.0
Day 2	18.5	1.8	Day 2	16.1	2.1	Day 2	12.7	1.0	Day 2	14.0	1.8
Day 3	15.0	3.4	Day 3	11.8	3.8	Day 3	10.8	0.4	Day 3	11.6	1.7
Day 4			Day 4			Day 4			Day 4		
Day 5	14.2	1.3	Day 5	13.6	0.3	Day 5	8.7	1.4	Day 5	12.9	1.5
Day 6	14.4	1.3	Day 6	15.3	0.8	Day 6	11.2	0.4	Day 6	12.9	0.8

Table 5.6: Summary of volumetric water content (θ) data from all sampling days. θ data represent the mean of 3 samples; standard deviations included. Day 4 10-30cm samples were lost.

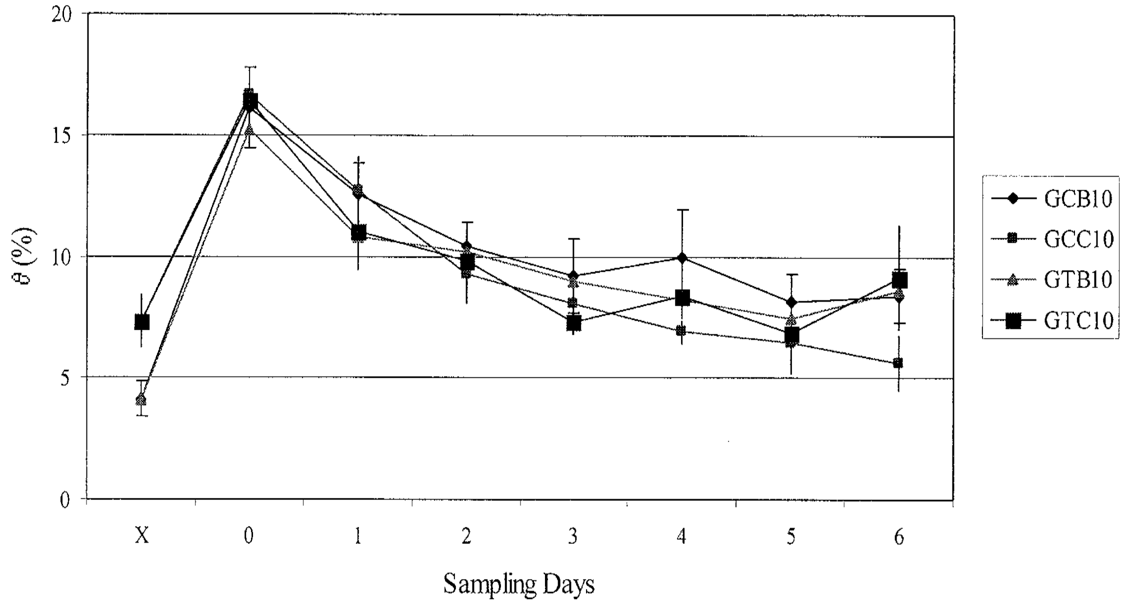

Figure 5.11: Time-series plot of θ for the grass ecosystem control and treatment plot soil samples from the 0-10cm soil depth interval. See **Table 5.1** for sample name legend.

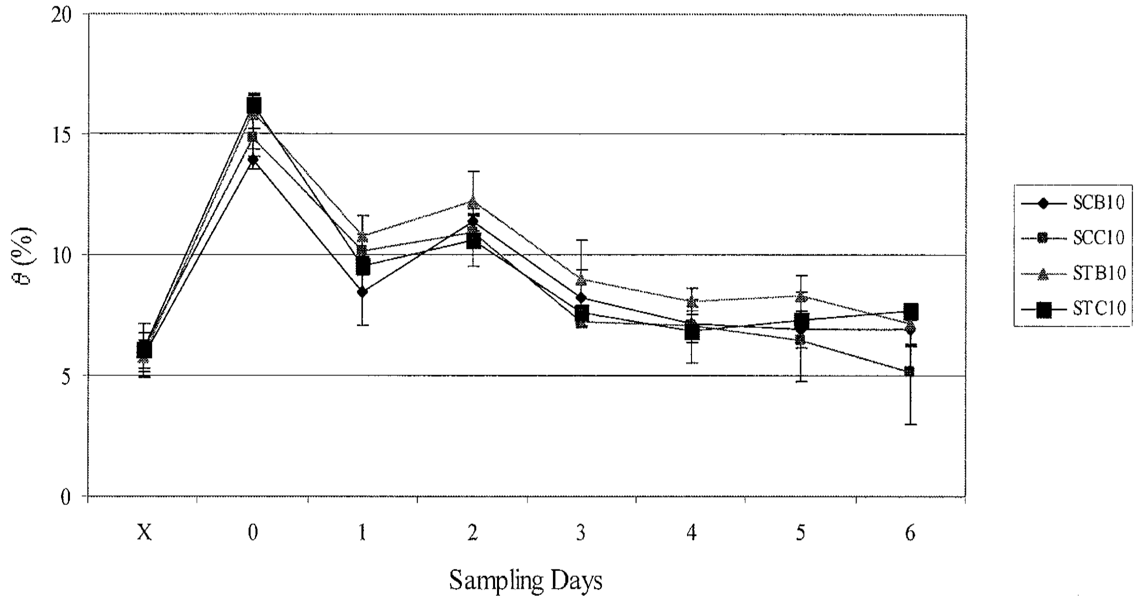

Figure 5.12: Time-series plot of θ for the shrub ecosystem control and treatment plot soil samples from the 0-10cm soil depth interval. See **Table 5.1** for sample name legend.

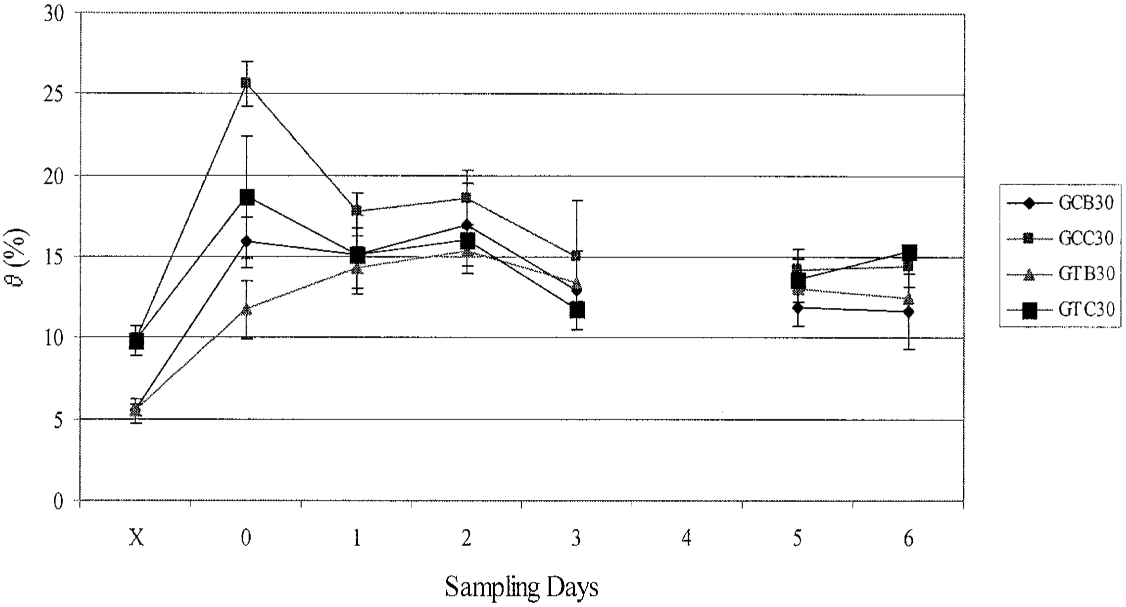

Figure 5.13: Time-series plot of θ for the grass ecosystem control and treatment plot soil samples from the 10-30cm soil depth interval. See **Table 5.1** for sample name legend. Day 4 soil samples were lost.

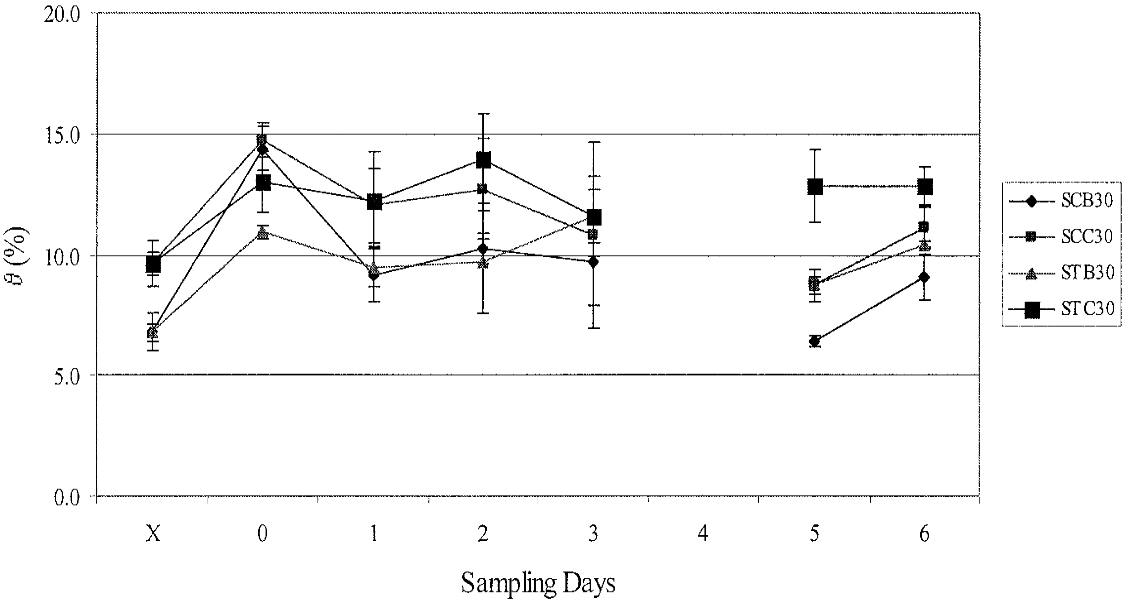

Figure 5.14: Time-series plot of θ for the shrub ecosystem control and treatment plot soil samples from the 10-30cm soil depth interval. See **Table 5.1** for sample name legend. Day 4 soil samples were lost.

6. DATA ANALYSIS AND INTERPRETATION

This chapter reviews and presents hypotheses with regard to the data presented in **Chapter 5.0: Soil Water Data**. The reader may need to refer to **Chapter 5.0: Soil Water Data** for referenced figures and tables.

6.1 Ecosystem Slopes Relative to MWL

Table 6.1 summarizes the slope from linear regressions of soil water $\delta^{18}O$ and $\delta^{2}H$ data on Day –X and Day 6. Control and treatment plot slopes are differentiated on Day 6 for each ecosystem. Refer to **Figure 5.3** through **Figure 5.8** for plots of this data relative to the MWL.

Sampling Day	Grass Ecosystem		Shrub Ecosystem	
	Control	*Treatment*	*Control*	*Treatment*
Day -X	2.2	-	1.8	-
Day 6	2.6	2.0	2.1	1.6

Table 6.1: Linear regression slope summary for soil water $\delta^{18}O$ and $\delta^{2}H$ data on Day – X and Day 6 for both ecosystems.

From **Table 6.1**, the slope is consistently lower for shrubs than grasses. In addition, the slope is consistently lower in the treatment plots than the control plots within each ecosystem. However, these observations are not statistically significant based on the comparison of the linear regression equations using t-tests. Two-tail t-tests with unequal variances were done for each slope comparison. If the P-value falls below 0.10 then any observed difference in the soil water slope is statistically significant. If the P-value falls above 0.10 then any observed difference in the soil water slope is not statistically significant. All comparisons yielded a P-value greater than 0.90 indicating very little statistical significance. Despite the lack of statistical significance, the numerical stable isotope balance model (**Chapter 7.0: STABLE ISOTOPE BALANCE MODEL**) provides some evidence that the observed slope may imply relative evaporation rates. For instance, the grass ecosystem control plot soil water $\delta^{18}O$ and $\delta^{2}H$ data on Day 6 shows from linear regression a slope of 2.6 while the treatment plot soil water $\delta^{18}O$ and $\delta^{2}H$ data on Day 6 shows from linear regression a slope of 2.0. The treatment plot shows a lower slope than the control plot. As a result, the evaporation rate may be higher in the treatment plot. The results from the numerical stable isotope balance model, in **Chapter 7.0: STABLE ISOTOPE BALANCE MODEL**, imply a lower slope may be associated with a higher evaporation rate. However, the model also demonstrates that transpiration can affect the slope.

6.2 Significance of ANOVA Results

Only two soil sampling localities based on ANOVA statistical methods yielded statistical significance (P-value < 0.10) on Day 6 from comparisons between control and treatment plots. **Table 6.2** summarizes the ANOVA statistics for those two Day 6 comparisons.

Soil Sampling Locality	Comparison	Ecosystem Process	P-Value
Grass Canopy Soil 0-10cm	Control vs. Treatment	Transpiration	0.077
Shrub Canopy Soil 0-10cm	Control vs. Treatment	Transpiration	0.006

Table 6.2: ANOVA statistics summary for the two comparisons that yielded statistical significance (P-value < 0.10). The column 'Ecosystem Process' assigns the presumed ecosystem process responsible for the statistical significance.

Transpiration is the presumed ecosystem process responsible for the statistical significance for the comparison of control and treatments plot shrub and grass 0-10cm canopy soil. Refer to **Figure 5.9** through **Figure 5.10** for plots of $\delta^{18}O$ soil water data on Day 0, Day 2 and Day 6 for each comparison discussed above. From qualitative inspection of **Figure 5.9** through **Figure 5.10**, the difference is clear by Day 6 that the $\delta^{18}O$ soil water data is statistically significant given the standard deviations on Day 6 do not overlap. The ANOVA statistics do not provide any information on to what extent the evaporation rate and/or transpiration rate are different between the control and treatment plots. However, we draw some qualitative conclusions in the following section. The statistical significance will be utilized in the application of the numerical stable isotope balance model (**Chapter 7.0**).

6.3 Control vs. Treatment: $\delta^{18}0$ and θ

Figure 6.1 shows the control and treatment plot $\delta^{18}O$ shrub canopy soil water data and canopy θ data for Day –X, Day 0, Day 2 and Day 6 from the 0-10cm soil depth interval. **Figure 6.2** shows the control and treatment plot $\delta^{18}O$ grass canopy soil water data and canopy θ data for Day –X, Day 0, Day 2 and Day 6 from the 0-10cm soil depth interval. The treatment plots for the shrub and grass canopy 0-10cm soils show on Day 6 a greater degree of enrichment from the initial $\delta^{18}O$ value than the control plots. The cause is presumably a result of a higher evaporation rate from the treatment plots than the control plots. The treatment plots show a higher θ than control plots on Day 6 with both plot types showing similar initial θ. A numerical stable isotope balance model was necessary to quantitatively estimate the evaporation and transpiration rates for each ecosystem (**Chapter 7.0: STABLE ISOTOPE BALANCE MODEL**).

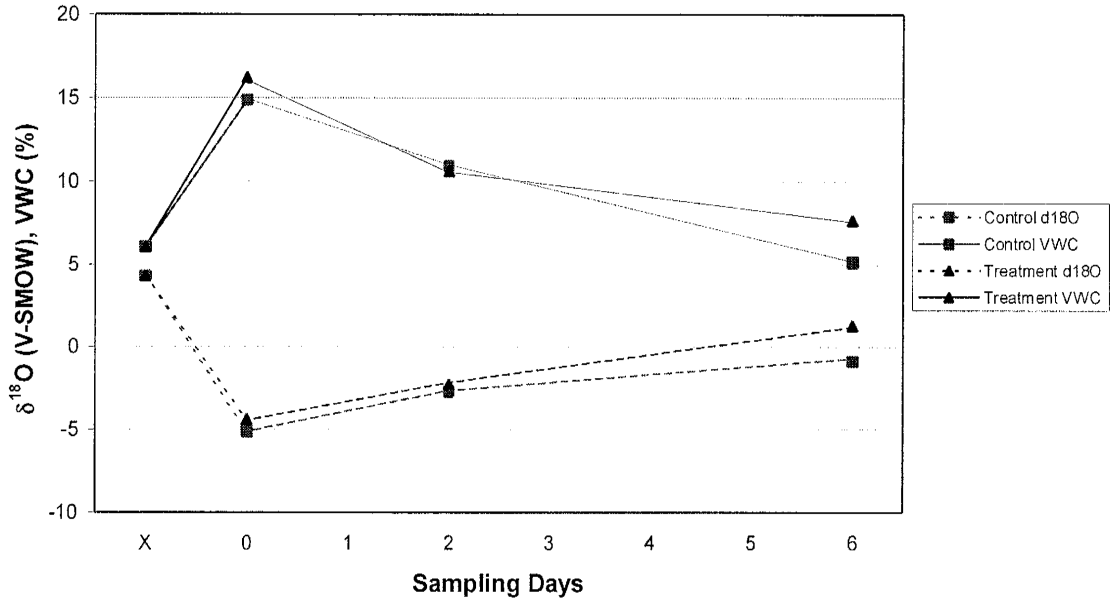

Figure 6.1: Control and treatment plot $\delta^{18}O$ soil water data and θ data for the shrub ecosystem, 0-10cm canopy soil. The points indicate the mean from three samples. The standard deviations are removed for clarity. Note: 'd18O' = '$\delta^{18}O$' in the legend.

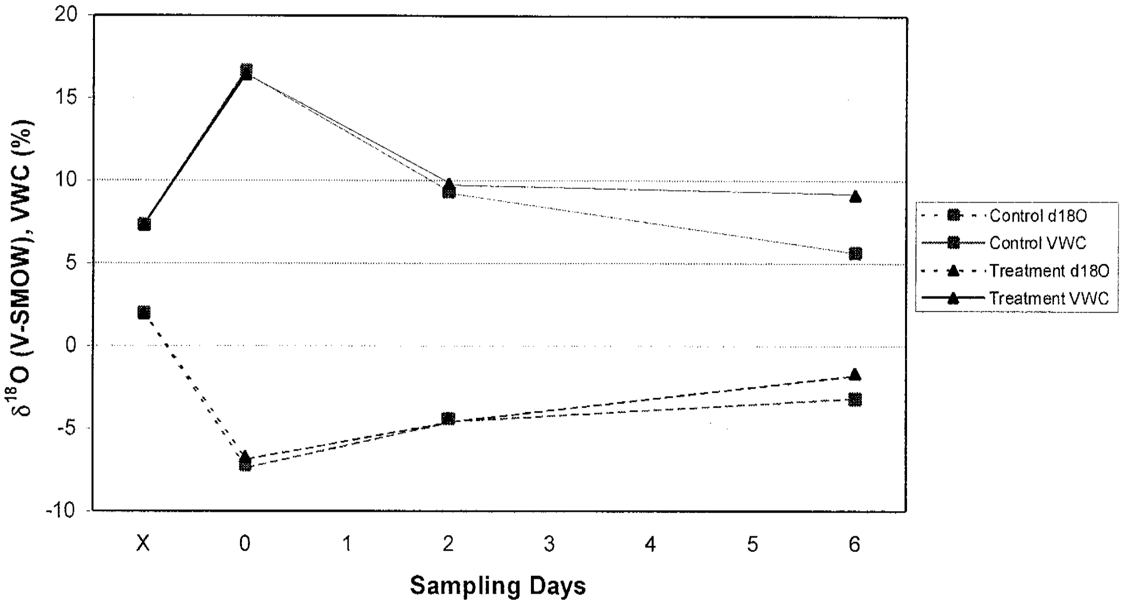

Figure 6.2: Control and treatment plot $\delta^{18}O$ soil water data and θ data for the grass ecosystem, 0-10cm canopy soil. The points indicate the mean from three samples. The standard deviations are removed for clarity. Note: 'd18O' = '$\delta^{18}O$' in the legend.

7. STABLE ISOTOPE BALANCE MODEL

This chapter describes the setup of a stable isotope balance model (model) and presents the results from the applications of the model. The model provides concurrent estimates of evaporation (E) and transpiration (T) rates from an initial soil water volume and initial $\delta^{18}O$ soil water value for the 0-10cm grass and shrub canopy soil. $\delta^{18}O$-enrichment of soil water, and evaporation and transpiration rates are setup in the model with continuous dependence on the amount of soil water available through time. The numerical method, Runge-Kutta Order Four (R-K, 4), was used to estimate the evaporation and transpiration rates since an analytical solution cannot be derived. R-K, 4 was applied to the initial $\delta^{18}O$ and θ soil water data from each soil sampling locality per plot per ecosystem to return evaporation and transpiration estimates on Day 2 and Day 6. We also present a check on the model through comparison of the model results to our soil physics estimates of the ET rate using the van Genuchten model (**van Genuchten, 1980**). Lastly, the ET rate will be partitioned into evaporation and transpiration based on the model results.

7.1 Model Setup, Solution Derivation and Numerical Methods

The post-precipitation soil water volume (V_s) changes as a function of time according to **Equation 7.1**:

$$\frac{dV_s}{dt} = -E - T \qquad (7.1)$$

The model assumptions inherent to **Equation 7.1** are that evaporation (E) and transpiration (T) are the only losses to the soil water volume over time. Furthermore, the model includes the assumption that infiltration to deeper soil layers (>10cm) ceases immediately after the precipitation event.

The isotopic evolution of a reservoir of soil water during evaporation and transpiration can be considered as analogous to the evolution of a closed-basin lake during evaporation. A governing equation analogous to Equation 2 in **Phillips et al. (1986)** can be formulated for the soil isotopic evolution problem, and is given below in **Equation 7.2**.

$$\delta_{vapor} = \frac{\delta_s - \varepsilon *}{\varepsilon * + 1} \qquad \textbf{(7.2)}$$

The model assumptions inherent to **Equation 7.2** are that the $\delta^{18}O$ value of transpired soil water is the same as the $\delta^{18}O$ value of soil water.

Recognizing the assumptions inherent to **Equation 7.1** and **Equation 7.2** and multiplying the equations into the form, $\frac{d(V_s \delta_s)}{dt}$, gives **Equation 7.3** by the chain rule:

$$\delta_S * \frac{dV_s}{dt} + V_s * \frac{d\delta_S}{dt} = -E * \left(\delta_{vapor}\right) - T * \delta_S \qquad \textbf{(7.3)}$$

The model is set up for derivation in **Equation 7.3** as an Initial Value Problem (IVP) for an Ordinary Differential Equation (ODE) with the initial condition, $\delta_S(0) = \delta_S^{\,o}$. An analytical solution can be derived from **Equation 7.1** with the initial condition, $V(0) = V_o$. The analytical solution is shown in **Equation 7.4**.

$$V_s(t) = V_0 + (-E - T) * t \tag{7.4}$$

Each term in **Equation 7.1** through **Equation 7.4** is defined as follows:

$\delta_s = \delta^{18}O$ of soil water [permil, $^o/_{oo}$]

$\delta_{vapor} = \delta^{18}O$ of soil water vapor [permil, $^o/_{oo}$]

V_s = soil water volume treated as an 'equivalent depth' [length, mm]

E = evaporation rate [length / time, mm/day]

T = transpiration rate [length / time, mm/day]

ε^* = enrichment factor for a liquid water and water vapor system which is based on temperature and adjusted for humidity (h) (**Gonfiantini, 1986**) as follows:

$$\varepsilon^* = \varepsilon_{LV} + 14.2 * (1 - h)$$

where ε_{LV} represents the enrichment factor based on temperature alone from **Equation 2.4** given $\varepsilon_{LV} = 1 - \alpha_{LV} * 10^3$. Air temperature and humidity are provided by SNWR meteorological stations.

Equation 7.1 and **Equation 7.4** can be substituted into the left-hand side of **Equation 7.3** and **Equation 7.2** can be substituted into the right-hand side of **Equation 7.3** to obtain the change of δ_s with time. However, an analytical solution could not be derived from **Equation 7.3** with **Equation 7.1, Equation 7.2** and **Equation 7.4** substituted appropriately, therefore the R-K, 4 method was used to approximate the of the form

appropriate

(7.5)

water

average

IVP. The R-K, 4 method approximates the solution y(t) to a problem of the form **(Burden and Faires, 2001)**:

$$\frac{dy}{dt} = f(t, y)$$

for $a \leq t \leq b$

with the initial condition:

$$y(a) = \alpha$$

Equation 7.5 is then setup for input into R-K(4) method after the appropriate substitutions from **Equation 7.1** and **Equation 7.4** into **Equation 7.3**:

$$\frac{d\delta_S}{dt} = \left[-E * \left(\frac{\delta_S(t) - \varepsilon}{\varepsilon + 1} \right) - T * \delta_S(t) - \delta_S(t) * (-E - T) \right] * \left[\frac{1}{\left(V_o + (-E - T) * t \right)} \right] \quad \textbf{(7.5)}$$

The following assumptions are inherent to the model:

i. Soil water extraction by plants (i.e. transpiration) is non-fractionating.

ii. Evaporation is fractionating.

iii. Evaporation and/or transpiration are the only losses to the soil water volume.

iv. Once the precipitation event ended, no additional inputs occurred.

v. The output evaporation rate and transpiration rate represent the average rates over the time evaluated during the numerical integration.

vi. No transpiration from intercanopy spaces. This assumption is based on ANOVA statistics and **Figure 1.2** (negligible root mass in intercanopy spaces).

vii. No transpiration from treatment plots.

7.2 Model Implementation and Results

The mean Day 0 $\delta^{18}O$ soil water and the mean Day 0 θ values were input into the model. The E and T values were then adjusted in the model until the model reproduced the Day 2 and Day 6 field $\delta^{18}O$ soil water value ranges. The model θ range did not match the field θ range in some cases. The range of field values (range based on standard deviations) versus the single (or mean) field value was reproduced with the model in order to assess the variability in the E and T rates necessary to produce the observed field values. As a result, a range of E and T rates is output from the model. T was set to zero in the model for the treatment plots and control plot intercanopy spaces. **Table 7.1** summarizes the Day 2 and Day 6 field and model θ and $\delta^{18}O$ ranges. **Table 7.2** summarizes the model E and T rate estimates. F in **Table 7.2** represents the fraction of soil water remaining on Day 2 and Day 6 as a result of E and T (**Equation 7.6**). F_E in **Table 7.2** represents the fraction of soil water remaining on Day 2 and Day 6 as a result of E only (**Equation 7.6**). F and F_E vary from 1 to 0.

$$F, F_E = \frac{V_t}{V_i} \qquad \textbf{(7.6)}$$

V_i represents the initial soil water volume immediately after the precipitation event and V_t represents the soil water volume some time after the precipitation event.

Sampling Locality	Day 2			
	Model $\delta^{18}O$ (‰)	Field $\delta^{18}O$ (‰)	Model θ (%)	Field θ (%)
GTC10	-4.6 to -4.2	-4.6 to -4.2	13.0 - 12.6	10.5 - 9.1
GCC10	-5.4 to -3.4	-5.4 to -3.4	10.5 - 8.1	10.5 - 8.1
GTB10	-0.7 to +2.1	-0.7 to +2.1	8.8 - 6.9	10.8 - 9.6
GCB10	-2.8 to +1.3	-3.5 to +1.3	16.1 - 6.8	11.3 - 9.5
STC10	-4.2 to -0.4	-4.2 to -0.4	15.4 - 9.1	11.7 - 9.5
SCC10	-3.4 to -2.0	-3.4 to -2.0	11.5 to 9.8	11.7 to 10.3
STB10	-1.4 to +3.2	-1.4 to +3.2	10.1 - 5.7	13.4 - 11.0
SCB10	-3.0 to +0.8	-3.0 to +0.8	10.2 - 7.1	11.9 - 10.9
Sampling Locality	**Day 6**			
	Model $\delta^{18}O$ (‰)	Field $\delta^{18}O$ (‰)	Model θ (%)	Field θ (%)
GTC10	-2.5 to -0.7	-2.5 to -0.7	11.4 - 9.9	11.4 - 7.0
GCC10	-3.9 to -2.5	-3.9 to -2.5	6.8 - 4.4	6.8 - 4.4
GTB10	+1.2 to +5.8	+1.2 to +5.8	6.3 - 5.4	9.7 - 8.3
GCB10	+1.0 to +4.8	+1.0 to +4.8	6.9 - 4.7	9.1 - 6.9
STC10	+0.7 to 1.9	+0.7 to 1.9	8.2 - 7.4	8.0 - 7.4
SCC10	-1.2 to -0.6	-1.2 to -0.6	5.3 - 4.9	5.3 - 4.9
STB10	+0.8 to +1.8	+0.8 to +1.8	7.3 - 6.5	8.0 - 6.2
SCB10	+1.0 to +4.6	+1.0 to +4.6	7.1 - 5.6	7.4 - 6.6

Table 7.1: Summary of the Day 2 and Day 6 field and model-generated θ and $\delta^{18}O$ ranges.

Sampling Locality	Day 2				Day 6			
	E (mm/day)	T (mm/day)	F (-)	F_E (-)	E (mm/day)	T (mm/day)	F (-)	F_E (-)
GTC10	1.73 - 1.96	0.00	0.79 - 0.76	0.79 - 0.76	0.95 - 1.18	0.00	0.66 - 0.58	0.66 - 0.58
GCC10	1.10 - 2.40	0.60 - 3.15	0.64 - 0.49	0.87 - 0.71	0.50 - 0.75	0.96 - 1.60	0.40 - 0.26	0.82 - 0.74
GTB10	3.22 - 4.18	0.00	0.58 - 0.45	0.58 - 0.45	1.48 - 1.63	0.00	0.42 - 0.36	0.42 - 0.36
GCB10	0.00 - 4.90	0.00	1.00 - 0.41	1.00 - 0.41	1.53 - 1.90	0.00	0.43 - 0.29	0.43 - 0.29
STC10	0.40 - 3.55	0.00	0.95 - 0.56	0.95 - 0.56	1.34 - 1.47	0.00	0.50 - 0.46	0.50 - 0.46
SCC10	1.60 - 2.55	0.00 - 0.70	0.77 - 0.67	0.79 - 0.66	0.77 - 0.86	0.74 - 0.92	0.36 - 0.33	0.69 - 0.65
STB10	2.90 - 5.10	0.00	0.64 - 0.36	0.64 - 0.36	1.43 - 1.56	0.00	0.46 - 0.41	0.46 - 0.41
SCB10	1.85 - 3.38	0.00	0.73 - 0.51	0.73 - 0.51	1.14 - 1.38	0.00	0.51 - 0.40	0.51 - 0.40

Table 7.2: Summary of Day 2 and Day 6 model evaporation and transpiration rate estimates using the R-K, 4 method. See **Table 5.1** for sample name notation.

7.3 Model Results Interpretation

The extreme variation of the model evaporation and transpiration rates from the Day 2 does not lend itself to easy interpretation and will not be evaluated (refer to **Chapter 9.0: 'Future Work'**). Recalling the focus of our discussion in **Chapter 6.3: 'Control vs. Treatment: $\delta^{18}0$ and θ'**, **Table 7.1** and **Table 7.2** contain data that offer insight into the peculiarity of the treatment plot soil waters showing more enrichment and higher soil water content than the control plot soil waters in 0-10cm canopy soils on Day 6. For the GTC10, the evaporation rate varied between 0.95 and 1.18 mm/day. Comparatively for the GCC10, the evaporation rate varied between 0.50 and 0.75 mm/day and the transpiration rate varied between 0.96 and 1.60 mm/day. The presence of significant transpiration was supported by the ANOVA statistics and is consistent with the high root density in canopy soil (**Figure 1.2**). Given the removal of plants and thus transpiration from the treatment plots, the E rate from the treatment plots was expected to be higher than the E rate from the control plots. The treatment plots have more soil water available for evaporation since T is absent. As the soil water content decreases, the E rate decreases (**Hornberger et al., 1998**). The treatment plot soil waters for both ecosystems were expected to show more stable isotope enrichment and a higher water content than control plot soil waters. However, it could not be anticipated if the E flux from the treatment plot would be less than the combined flux of E and T from the control plots. The model results show that the E rate from the treatment plots was higher than the control plots for both ecosystems. The water content, however, remained higher in the treatment plots because the control plots had additional soil water loss due to transpiration. The level of stable isotope enrichment does not depend only on total soil water loss. The greater level of stable isotope enrichment in the treatment plots is due to the fraction of soil water loss by evaporation being greater in the treatment plots than the control plots.

Similar conclusions can be drawn for the shrub ecosystem. For the STC10, the evaporation rate varies between 1.34 and 1.47 mm/day. Comparatively for the SCC10, the evaporation rate varies between 0.77 and 0.86 mm/day and the transpiration rate varied between 0.74 and 0.92 mm/day.

The model evaporation rates from the control and treatment 0-10cm intercanopy spaces in each ecosystem confirm the assessment made with the ANOVA statistics. The evaporation rates are approximately the same from control and treatment plot intercanopy spaces. For the GTB10, the evaporation rate varies between 1.48 and 1.63 mm/day. Comparatively for the GCB10, the evaporation rate varies between 1.53 and 1.90 mm/day. In addition, the F values are approximately the same, 0.43-0.29 for the control plot and 0.42-0.36 for the treatment plot. The amount of soil water volume lost due to transpiration from intercanopy space in the grass ecosystem can be neglected. For the STB10, the evaporation rate varies between 1.43 and 1.56 mm/day. Comparatively for the SCB10, the evaporation rate varies between 1.14 and 1.38 mm/day. In addition, the F values are approximately the same, 0.51-0.40 for the control plot and 0.46-0.41 for the treatment plot. The amount of soil water volume lost due to transpiration from intercanopy space in the shrub ecosystem can be neglected.

7.4 Model Testing and ET Partitioning

As a check on the model, soil E rates were estimated based on independent θ data provided from TDR probes placed in the soil at each meteorological station in the SNWR. **Bhark (2002)** measured the saturated water content (θ_{sat}) and residual water content (θ_{res}) with the field TDR probes for each soil type evaluated in this study. θ and matric-potential (h) were then measured simultaneously in laboratory columns to develop soil moisture retention curves. Once the curves were developed, van Genuchten parameters (α, n and m) were fitted (**van Genuchten, 1980**). Van Genuchten formulations, **Equation 7.5** and **Equation 7.6,** were employed to estimate matric potential gradients, unsaturated hydraulic conductivity (K(θ)) and soil water fluxes from θ data.

$$\theta = \theta_{res} + \frac{(\theta_{sat} - \theta_{res})}{\left(1 + (h * \alpha)^n\right)^m} \tag{7.5}$$

$$K(\theta) = K_{sat} * \left(\frac{\theta - \theta_{res}}{\theta_{sat} - \theta_{res}}\right)^{0.5} * \left(1 - \left(1 - \left(\frac{\theta - \theta_{res}}{\theta_{sat} - \theta_{res}}\right)^{\frac{1}{m}}\right)^m\right)^2 \tag{7.6}$$

The TDR probes collected θ data every 0.5 hour and were placed at 2.5cm, 12.5cm and 22.5cm below the soil surface. Given the θ data for the period of interest in this study and the ability to estimate h and K(θ) from θ, ET rates were estimated as the measured flux from 12.5cm to 2.5cm with the following unsaturated flow equation (**Equation 7.7**):

$$\frac{d\theta}{dt} = -\nabla \bullet \vec{q} \qquad \textbf{(7.7)}$$

For the one-dimensional vertical flux, **Equation 7.7** can be written as shown in **Equation 7.8**:

$$\frac{d\theta}{dt} = \frac{-d\left(K(\theta) * \left(\frac{dh}{dz} + 1\right)\right)}{dz} \qquad \textbf{(7.8)}$$

The upward gradients measured in the soil are a result of evaporation and transpiration. The soil gradients can only be used to estimate the E rate from the soil. A separate gradient exists within the plant between the soil and the atmosphere. However, the estimated flux from the soil gradients will be referred to as ET fluxes given the gradient resulted from E and T soil water losses. Based on **Equation 7.8** and the measured θ datae, the average ET rate for the shrub ecosystem over the course of 6 days after the precipitation event was 1.42 mm/day. The average ET rate for the grass ecosystem over the course of 6 days after the precipitation event was 2.21 mm/day. The meteorological station in the grass ecosystem experienced a power failure after Day 4. Day 5 and Day 6 ET estimates for the grass ecosystem were extrapolated from a simple interpolated polynomial for the Day 0 to Day 4 ET estimates. These ET values will be shown to reasonably agree with the numerical stable isotope balance model ET estimates developed below.

The range of model evaporation and transpiration were weighted with respect to the surface cover statistics as shown in **Figure 7.1** to estimate average ecosystem ET. ET was estimated as shown in **Equation 7.9**.

$$ET = (E_c+T_c)*X+(E_i+T_i)*Y \quad \textbf{(7.9)}$$

where X represents the proportion of canopy surface cover and Y represents the proportion of intercanopy space surface cover. The subscript 'c' and 'i' represent canopy and intercanopy space, respectively. The %E and %T were estimated using a similar equation (**Equation 7.10**); the %E calculation is shown.

$$\%E = (E_c*X + E_i*Y) / ET \quad \textbf{(7.10)}$$

Table 7.3 summarizes our ET estimates as well as %E and %T based on the model results. The results agree very well with the estimates provided by the 1-D, unsaturated flow equation mentioned previously. The grass ecosystem provides an ET range of 1.49 to 2.15 mm/day from the model with the unsaturated flow equation providing an ET rate of 2.21 mm/day (**Figure 7.2**). The shrub ecosystem provides an ET range of 1.25 to 1.50 mm/day from the model with the unsaturated flow equation providing an ET rate of 1.42 mm/day (**Figure 7.3**). From **Table 7.3**, the %E in the shrub ecosystem (79-84%) is higher than the grass ecosystem (52-70%) but the %T in the grass ecosystem (30-48%) is higher than the shrub ecosystem (16-21%). Six days after the precipitation event, these figures translate into 9.0 to 13 mm of soil water transpired by the grasses, while the shrubs transpired 7.5 to 9.0 mm of soil water.

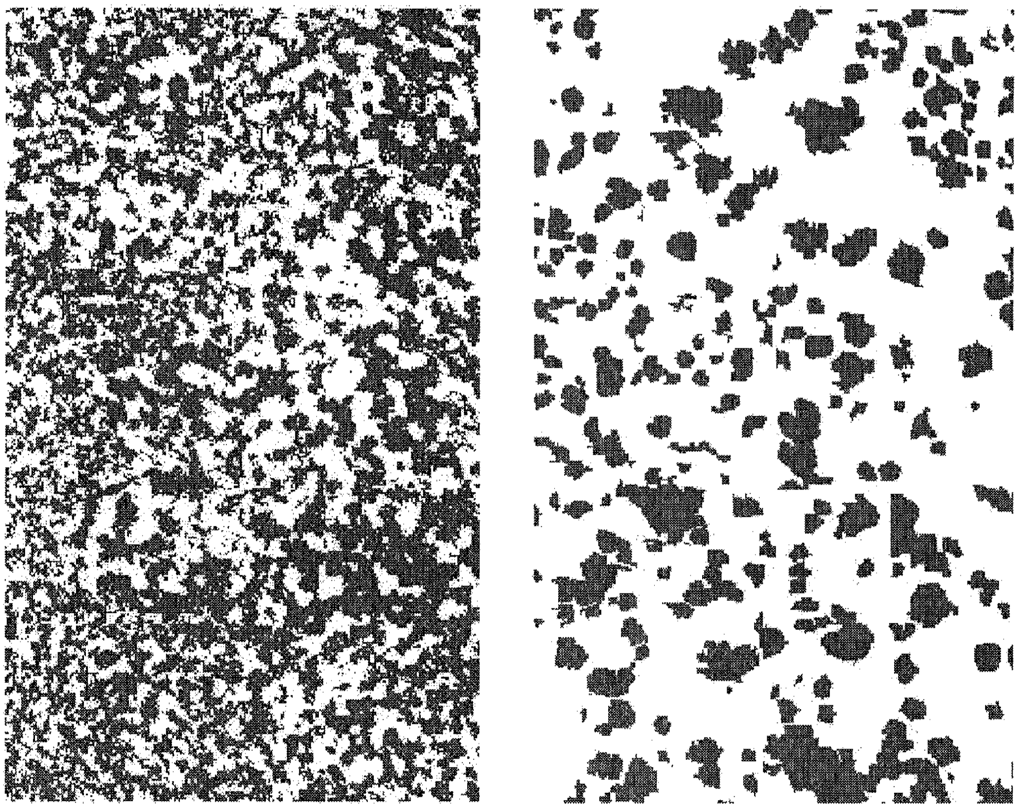

GRASS **SHRUB**

Figure 7.1: Mosaic of surface cover from digital overhead photo survey conducted during January 2002. The gray regions represent the canopy surface cover, while the white regions indicate the intercanopy space surface cover. Surface dimensions were 15m by 25m. The grass canopy occupies 55% of the surface while the grass intercanopy space occupies 45% of the surface. The shrub canopy occupies 70% of the surface while the shrub intercanopy space occupies 30% of the surface.

Ecosystem	Isotope Model ET (mm/day)	van Genuchten Model ET (mm/day)	E (%)	T (%)	T (mm)	E:T
Grass	1.49 - 2.15	2.21	52 - 70	30 - 48	9.0 - 13.0	1:1 to 7:3
Shrub	1.25 - 1.50	1.42	79 - 84	16 - 21	7.5 - 9.0	15:4 to 21:4

Table 7.3: Isotope model and van Genuchten model ET estimates. %E, %T and E:T were weighted with respect to ecosystem surface cover statistics (**Figure 7.1**). T is the total post-precipitation soil water loss due to transpiration, in equivalent depth units.

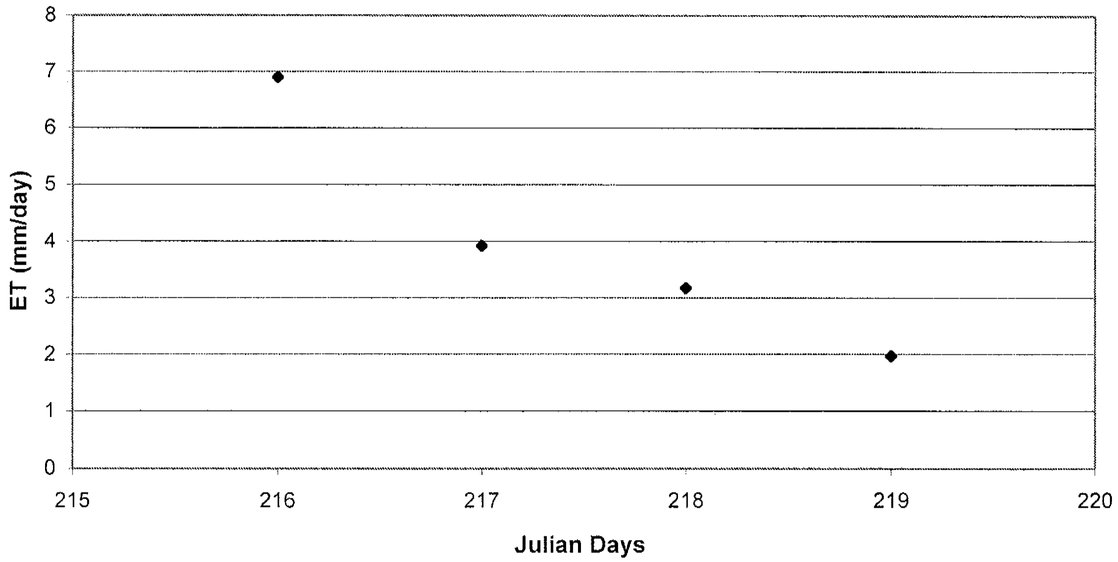

Figure 7.2: ET estimates from 1-D van Genuchten model (**Equation 7.8**) for the grass ecosystem. The average ET rate over six days, given an interpolated estimate of ET for Julian Day 221 and 222, is 2.21 mm/day.

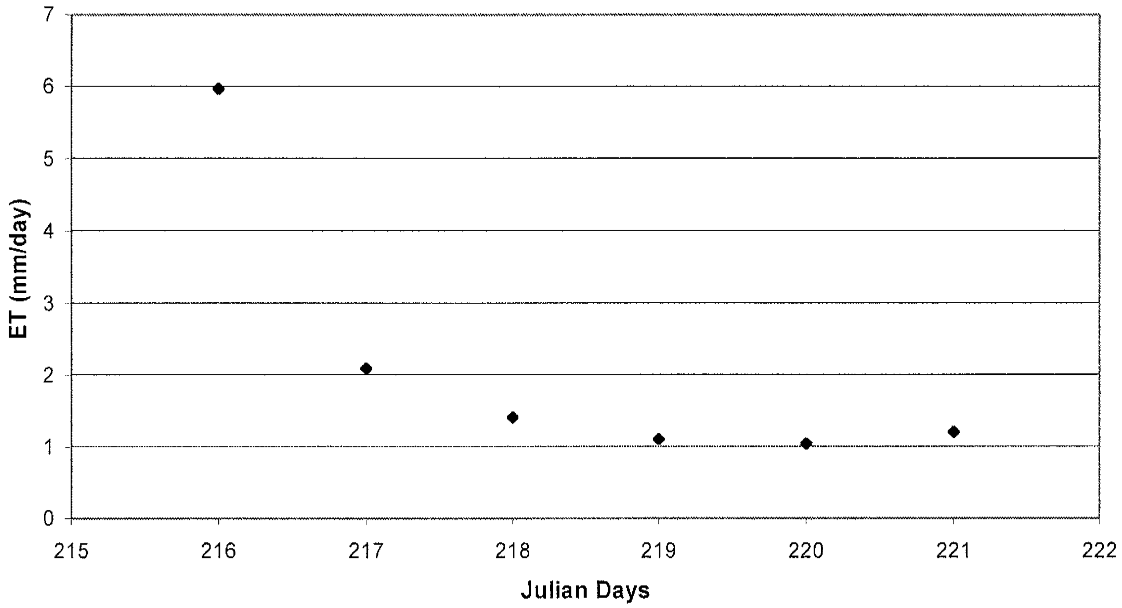

Figure 7.3: ET estimates from 1-D van Genuchten model (**Equation 7.8**) for the shrub ecosystem. The average ET rate over six days is 1.42 mm/day.

8. CONCLUSIONS

The stable isotope balance model estimated the ET rate quite favorably compared to an independent estimate of ET using a 1-D unsaturated flow model (**Table 7.3**); therefore we accept the evaporation and transpiration rate estimates predicted by the model (**Table 7.1**). However, the evaporation and transpiration rates estimates from Day 6 are more reliable than those from Day 2. By Day 6, the bulk soil water losses and net effects on the θ and $\delta^{18}O$ are a result of evaporation and transpiration only. Up to Day 2, other processes such as flow to greater soil depths or general soil water redistribution as a result of the precipitation event may be the cause for the relatively high variability of evaporation and transpiration rates on Day 2. In addition, there may be other processes involved that are not captured by the stable isotope balance model between Day 0 and Day 2.

The extraction of soil water by plants (i.e. transpiration) has been shown to be non-fractionating (**Zimmerman et al., 1967**). The results from the stable isotope balance model showed that transpiration, although non-fractionating during soil water extraction by plants, influences the stable isotope enrichment of soil water by limiting the amount of soil water available for evaporation. The evaporation rate has been conventionally estimated from soil water stable isotope data alone (**Barnes and Allison, 1983**). The transpiration rate cannot be estimated from stable isotope data alone. The transpiration rate can be estimated from the initial and final stable isotope and water content data using the stable isotope balance model. The model $\delta^{18}O$ and θ 0-10cm canopy soil water data on Day 6 showed that more enrichment of soil water from an initial $\delta^{18}O$ value, which is typically associated with a higher evaporation rate, does not necessarily mean a lower θ (**Figure 6.1 and Figure 6.2**). As shown by our stable isotope balance model, the transpiration rate can lower the θ, thus the evaporation rate becomes lower as evidenced by the less enrichment. The treatment plot soil waters showed more stable isotope enrichment and higher water content than the control plot soil waters. The model results show that the evaporation rate from the treatment plots was higher than the control plots for both ecosystems. The water content remained higher in the treatment plots because the control plots had additional soil water loss due to transpiration. The level of stable isotope enrichment does not depend only on total soil water loss. The greater level of stable isotope enrichment in the treatment plots is due to the fraction of soil water loss by evaporation being greater in the treatment plots than the control plots.

Of the total post-precipitation soil water loss in the shrub ecosystem, 16-21% was transpired by the shrubs and 79-84% was evaporated. Of the total post-precipitation soil water loss in the grass ecosystem, 30-48% was transpired by the grasses and 52-70% was evaporated. Six days after the precipitation event, these figures translate into 9.0 to 13 mm of soil water transpired by the grasses, while the shrubs transpired 7.5 to 9.0 mm of soil water. This study shows that the shrubs do not have an advantage over grasses, with respect to removing soil moisture that infiltrates following a typical wet-season precipitation event. Additional work is necessary to assess how the contrasts in water use between grasses and shrubs varies throughout the year, and how this contributes to the long term changes in ecosystem structure associated with the shrub encroachment.

9.0 FUTURE WORK

Our stable isotope balance model can be expanded to include the effects of soil diffusion on stable isotope transport during evaporation and transpiration, and other processes such as infiltration to greater soil depths, lateral soil water redistribution from canopy to intercanopy space as shown in **Bhark (2002)**, and the net downward diffusion of stable isotopes of the soil water molecule as shown in **Barnes and Allison (1983)**. We expect that such expansion would help to refine or reduce the variability of the Day 2 evaporation and transpiration estimates and develop a better understanding of the influence of evaporation and transpiration on soil at greater depths, in particular the 10-30cm soil depth interval. The number of soil samples could also be increased to reduce the standard deviations associated with the soil water $\delta^{18}O$ and θ data. This might allow for better detection of transpiration rates from the intercanopy space if ANOVA statistics are used.

REFERENCES

Bahre, C. J. (1991) A Legacy of Change: Historic Human Impact on Vegetation of the Arizona Borderlands. Tucson: Univ. Ariz. Press.

Barnes, C. J., and Allison, G.B. (1983). "The distribution of deuterium and ^{18}O in dry soil. Theory." Journal of Hydrology **60**: 141-156.

Bhark, E. W. (2002). Water Availability to Vegetation Across a Semiarid Shrubland and Grassland Ecotone, Sevilleta Wildlife Refuge, New Mexico. M.S. Thesis Department of Earth and Environmental Science. Socorro, New Mexico, New Mexico Institute of Mining & Technology: p.77.

Bhark, E. W. and Small, E. E., (2003). "Association between plant canopies and the spatial patterns of infiltration in shrubland and grassland of the Chihuahuan desert." Ecosystems, **6**:185-196.

Bottinga, Y., (1968). "Calculation of fractionation factors for carbon and oxygen exchange in the system calcite carbon dioxide water." Journal of Physical Chemistry **72**: 800-808.

Buffington, L. D., and Herbel, C.H. (1965). "Vegetational changes on a semidesert grassland range from 1958 to 1963." Ecological Monogram **35**: 139-164.

Burden, R. and Faires, J.D. (2001). Numerical Analysis. 7th edition, Brooks/Cole.

Campbell, A. R., Phillips, F.M., and Vanlandingham, R.J. (1995). "Stable isotope study of soil water, WIPP Site New Mexico: Estimation of recharge to rustler aquifers." Radioactive Waste Management and Environmental Restoration **19**: 1-13.

Campbell, A. R., and Larson, P.B. (1998). Introduction to stable isotope applications in hydrothermal systems. In Techniques in Hydrothermal Ore Deposits. P. B. Richards and Larson, eds., Society of Economic Paleontologists and Mineralogists. **10:** 173-193.

Chapman, J. B., Ingraham, N.L., and Hess, J.W. (1992). "Isotopic investigations of infiltration and unsaturated zone flow processes at Carlsbad Cavern, New Mexico." Journal of Hydrology **133**: 343-363.

Coleman, M. C., Shepard,T.J., Durham, J.J., Rouse, J.D., and Moore, G.R. (1982). "Reduction of water with zinc for hydrogen isotope analysis." Analytical Chemistry **54**: 993-995.

Craig, H. (1961). "Isotopic variations in meteoric waters." Science **133**: 1702-1703.

Criss, R. E. (1999). Principles of Stable Isotope Distribution. New York Oxford, Oxford University Press.

Friedman, M., and O'Neil, J.R. (1977). Compilation of stable isotope fractionation factors of geochemical interest. Data of Geochemistry; USGS Professional Paper 440-KK.

Friedman, I., Smith, G.I., Gleason, J.D., Warden, A., and Harris, J.M. (1992). "Stable isotope composition of waters in southeastern California: 1. Modern Precipitation." Journal of Geophysical Research **97**: 5795-5812.

Gardner, W. H. (1986). Water Content. Methods of soil analysis. Part 1. Physical and mineralogical methods. A. Klute. Madison, WI, American Society of Agronomy.

Gonfiantini, R., 1986. Environmental isotopes in lake studies. In: P. Fritz and J.C. Fontes (Eds), Handbook of Environmental Isotope Geochemistry, Vol. 2. Elsevier Scientific, Amsterdam, Netherlands, pp. 113-167.

Hayes, J. M. (1983). Practice and principles of isotopic measurements in organic geochemistry. Organic Geochemistry of Contemporaneous and Ancient Sediments. W. G. Meinschein, ed.,. Bloomington, IN, Society of Economic Paleontologists and Mineralogists: 5-31.

Hennessy, J. T., Gibbens, R.P., Tromble, J.M. and Cardenas, M. (1983). "Vegetation changes from 1935 to 1980 in mesquite dunelands and former grasslands of southern New Mexico." Journal of Range Management **36**: 370-374.

Hornberger, G. M., Raffensperger, J. P., Wiberg, P. L. and Eshleman, K. N. (1998). Elements of Physical Hydrology. John Hopkins University Press, Baltimore.

Hsieh, et al., (1998). "Oxygen isotopic composition of soil water: quantifying evaporation and transpiration." Geoderma 82: 269-293.

Humphrey, R. R. (1958) "The desert grassland: a history of vegetational change and an analysis of causes." Bot. Rev. **24**: 193-252.

Inglis, J. M. (1964) A History of Vegetation on the Rio Grande Plain. Austin: Texas Parks Wildlife Department.

Kendall, C., and Coplen, T.B. (1985). "Multisample conversion of water to hydrogen by zinc for stable isotope determination." Analytical Chemistry **1985**: 1437-1446.

Kieft, T. L., White, C.S., Loftin, S.R., Aguilar, R., Craig, J.A., and Skaar, D.A. (1998). "Temperal dynamics in soil carbon and nitrogen resources at a grassland-shrubland ecotone." Ecology **79**: 671-683.

Majoube, M. (1971). "Fractionnement en oxygene 18 et en deuterium entre l'eau et sa vapeur." Journal of Chemical Physics **18**: 1425-1436.
Moore, D. S., and McCabe, G.P. (2003). Introduction to the Practice of Statistics. New York, W.H. Freeman and Company.

Neilson, R. P. (1986). "High resolution climatic analysis and southwest biogeography." Science **232**: 27-34.

Phillips, F.M., Person, M.A., and Muller A.B. (1986). "A numerical model for simulating the isotopic evolution of closed-basin lakes." Journal of Hydrology **85**: 73-86.

Schlesinger, W. H., Reynolds, J. F., Cunningham, G. L., Huenneke, L. F., Jarrell, W. M., Virginia, R. A. and Whitford, W. G. (1990). "Biological Feedbacks in Global Desertification." Science **247**: 1043-1048.

Small, E. E. and Kurc, S., (2003), "Tight coupling between soil moisture and the surface radiation budget in semiarid environments: Implications for land-atmosphere interactions." Water Resources Research, 39. 4, 10, 1278.

Shurbaji, A. R. M. (1994). The contribution of $H_2{}^{18}O$, ^{2}HHO, and Cl^- to the modeling of water movement in the unsaturated zone. PhD Dissertation Department of Geoscience. Socorro, NM, New Mexico Institute of Mining & Technology: p. 150.

Socki, R. A., Karlsson, H.R., and Gibson, E.K. (1992). "Extraction technique for the determination of oxygen-18 in water using pre-evacuated glass vials." Analytical Chemistry **64**: 829-831.

Thompson, S. K. (1992). Sampling. New York, Wiley.

Urey, H. C. (1947). "The thermodynamic properties of isotopic substances." Journal of Chemical Society, London: 562-581.

van Genuchten, M. Th., (1980) "A closed-form equation for predicting the hydraulic conductivity of unsaturated soil." Journal of the Soil Science Society of America, 44: 892-898.

Walker, F. W., Parrington, J.R., and Feiner, F. (1989). Nuclides and Isotopes. San Jose, California, General Electric Co.

Weltzin, J. F., Loik, M. E., Schwinning, S., Williams, D. G., Fay, P. A., Haddad, B. M., Harte, J., Huxman, T. E., Knapp, A. K., Lin, G., Pockman, W. T., Shaw, R., Small, E. E., Smith, M. D., Smith, S. D., tissue, D. T., Zak, J. C., 2003, Assessing the response of terrestrial ecosystems to potential changes in precipitation, Bioscience, 53, 10: 941-952.

York, J. C., and Dick-Peddie, W.A. (1969). Vegetation changes in southern New Mexico during the past one hundred years. Arid Lands in Perspective. W. G. McGinnes, and Goldman, B.J., eds., Tucson, University of Arizona: 155-166.

Zimmermann, U., Ehhalt, D., and Munnich, K.O. (1967). Soil water movement and evapotranspiration: changes in the isotopic composition of the water. Proceedings of the Symposium on Isotopes in Hydrology. Vienna, International Atomic Energy Agency (I.A.E.A.): 567-584.

APPENDIX I: δ-DATA

Appendix I: δ-Data, Day -X							
*Date:	9/17,23/2002						
*Computer identifies Sept 17th-18th; Sept 23rd-24th							
9/17/02	$\delta^{13}C$		$\delta^{18}O$		Temp:	34.1°C	Begin: 11am
Standards	Delta-Mean	Std. Dev.	Delta-Mean	Std. Dev.	Correction:	**38.890**	End: 6pm
Zero Enrich	0.005	0.01	0.001	0.027			
Big Tank	0.002	0.027	-0.042	0.05			
STD-STD	-3.549	0.03	24.797	0.041			
CO_2-8	-3.564	0.029	24.784	0.02			
RE53-02-46619	-4.223	0.043	25.512	0.050			
RE53-02-46619 dup	-4.318	0.032	25.563	0.038			
		corrected:	-13.39				
9/23/02	$\delta^{13}C$		$\delta^{18}O$		Temp:	33°C	Begin: 11am
Standards	Delta-Mean	Std. Dev.	Delta-Mean	Std. Dev.	Correction:	**38.580**	End: 7pm
Zero Enrich	0.012	0.098	-0.06	0.092			
Zero Enrich	0.016	0.127	-0.06	0.151			
Zero Enrich	0.038	0.041	-0.003	0.096			
Zero Enrich	0.007	0.035	-0.053	0.038			
STD-STD	-3.552	0.03	24.816	0.020			
CO_2-8	-3.571	0.016	24.799	0.074			
RE53-02-46619	-4.189	0.035	25.846	0.037			
		corrected:	-13.044				
	$\delta^{13}C$		$\delta^{18}O$				
Samples	vs. PDB	Std. Dev.	vs. VSMOW	Std. Dev.	Corrected $\delta^{18}O$	Mean	Std. Dev.
SOIL							
XGB10A	-4.599	0.034	53.914	0.058	15.024	14.593	1.452
XGB10B	-4.448	0.032	51.864	0.052	12.974		
XGB10C	-4.475	0.016	54.671	0.040	15.781		
XGB30A	-4.811	0.048	49.608	0.055	10.718	11.072	0.653
XGB30B	-4.433	0.041	49.563	0.067	10.673		
XGB30C	-4.391	0.025	50.716	0.050	11.826		
XGB30C dup	-4.37	0.017	50.478	0.041	11.588		
XGC10A	-5.021	0.037	42.006	0.058	3.116	1.955	1.027
XGC10B	-4.473	0.042	40.056	0.070	1.166		
XGC10C	-5.755	0.033	40.473	0.082	1.583		
XGC10B dup	-4.484	0.029	39.945	0.066	1.055		
XGC30A	-4.675	0.053	42.459	0.064	3.569	1.762	2.029
XGC30B	-4.464	0.042	38.457	0.064	-0.433		
XGC30C	-4.461	0.029	41.041	0.077	2.151		
XGC30A dup	-4.606	0.02	42.558	0.058	3.668		
XSB10A	-5.278	0.014	52.48	0.076	13.590	12.962	2.228
XSB10B	-4.599	0.037	49.378	0.075	10.488		
XSB10C	-4.537	0.031	53.699	0.054	14.809		
XSB30A	-4.49	0.035	47.435	0.035	8.545	8.898	1.484
XSB30B	-4.376	0.017	46.513	0.062	7.623		
XSB30C	-6.336	0.047	49.417	0.062	10.527		
XSC10A	-4.45	0.035	43.53	0.061	4.640	4.293	0.369
XSC10B	-4.462	0.022	43.222	0.037	4.332		
XSC10C	-4.996	0.038	42.796	0.058	3.906		
XSC10A dup	-4.42	0.041	43.604	0.066	4.714		
XSC30A	-5.044	0.032	43.777	0.077	5.197	4.205	1.499
XSC30B	-4.321	0.03	43.518	0.031	4.938		
XSC30C	-4.329	0.079	41.061	0.080	2.481		
XSC30A dup	-5.06	0.027	43.853	0.040	5.273		

Appendix I: δ-Data, Day -X

9/5/02	δ^2H			H_3	Correction Equation:	
Standards	Delta-Mean	Std. Dev.		33.190	1.0227*X + 4.6017	
STD-STD	-127.26	0.247				
STD-STD dup	-126.981	0.199				
2/12/03	δ^2H			H_3	Correction Equation:	
Standards	Delta-Mean	Std. Dev.		51.324	1.0112*X + 5.13	
Zero Enrich	-0.483	0.363				
Zero Enrich dup	-0.698	0.16				
STD-STD	-50.653	0.152				
STD-STD dup	-50.781	0.264				
NM-2	-99.962	0.376				
	δ^2H					
Samples	vs. SMOW	Std. Dev.	Corrected δ^2H	Mean	Std. Dev.	
XGB10A	-12.424	0.32	-8.1043248	-13.820	6.231	
XGB10B	-24.508	0.24	-20.4626316			
XGB10C	-17.106	0.385	-12.8926062			
XGB30A	-23.199	0.247	-19.1239173	-19.711	3.362	
XGB30B	-27.31	0.364	-23.328237			
XGB30C	-20.81	0.19	-16.680687			
XGC10A	-44.668	0.214	-41.0802636	-45.071	3.456	
XGC10B	-50.541	0.303	-47.0865807			
XGC10C	-50.501	0.33	-47.0456727			
XGC30A	-34.641	0.225	-30.8256507	-36.805	6.958	
XGC30B	-47.955	0.444	-44.4418785			
XGC30C	-38.868	0.297	-35.1486036			
XGC30A dup	-34.911	0.444	-31.1017797			
XSB10A	-17.983	0.404	-13.7895141	-14.722	4.376	
XSB10B	-23.555	0.388	-19.4879985			
XSB10C	-15.145	0.209	-10.8870915			
XSB30A	-33.289	0.371	-28.5318368	-27.066	3.854	
XSB30B	-34.713	0.235	-29.9717856			
XSB30C	-27.516	0.212	-22.6941792			
XSB30A dup	-32.641	0.149	-27.8765792			
XSC10A	-36.931	0.505	-33.1676337	-32.508	0.886	
XSC10B	-36.626	0.455	-32.8557102			
XSC10C	-35.302	0.524	-31.5016554			
XSC30A	-34.269	0.128	-29.5228128	-29.714	1.509	
XSC30B	-33.069	0.16	-28.3093728			
XSC30C	-36.036	0.242	-31.3096032			

Appendix I: δ-Data, Day 0							
*Computer identifies 09/24 & 10/02,03 & 10/15,16 & 10/30							
9/24/03	$\delta^{13}C$		$\delta^{18}O$		Temp:	34.5°C	Begin: 10am
Standards	Delta-Mean	Std. Dev.	Delta-Mean	Std. Dev.	Correction:	**38.300**	End: 6pm
Zero Enrich	0.012	0.098	-0.06	0.092			
Big Tank	0.007	0.035	-0.053	0.038			
STD-STD	-3.552	0.03	24.816	0.02			
CO_2-8	-3.571	0.016	24.799	0.074			
RE53-02-46619	-4.189	0.035	25.846	0.037			
		corrected:	-12.454				
10/02,03/2003	$\delta^{13}C$		$\delta^{18}O$		Temp:	34.5°C	Begin:11am
Standards	Delta-Mean	Std. Dev.	Delta-Mean	Std. Dev.	Correction:	**38.300**	End: 5:30pm
Zero Enrich	0.027	0.041	-0.008	0.051			
Big Tank	0.011	0.031	-0.053	0.039			
STD-STD	-3.555	0.056	24.804	0.047			
CO_2-8	-3.564	0.039	24.724	0.073			
RE53-02-46619	-4.375	0.044	25.522	0.053			
		corrected:	-12.778				
10/15,16/2003	$\delta^{13}C$		$\delta^{18}O$		Temp:	34°C	Begin: 11am
Standards	Delta-Mean	Std. Dev.	Delta-Mean	Std. Dev.	Correction:	**38.390**	End: 7pm
Zero Enrich	-0.032	0.034	-0.003	0.067			
Big Tank	-0.006	0.04	-0.013	0.037			
STD-STD	-3.554	0.037	24.813	0.05			
CO_2-8	-3.533	0.04	24.803	0.056			
RE53-02-46619	-4.08	0.025	25.955	0.088			
		corrected:	-12.435				
10/30/03	$\delta^{13}C$		$\delta^{18}O$		Temp:	31.5°C	Begin: 11am
Standards	Delta-Mean	Std. Dev.	Delta-Mean	Std. Dev.	Correction:	**38.870**	End: 6pm
Zero Enrich	0.007	0.022	-0.01	0.045			
Big Tank	0.005	0.024	-0.011	0.092			
STD-STD	-3.521	0.01	24.718	0.042			
CO_2-8	-3.525	0.019	24.765	0.061			
RE53-02-46619	-4.24	0.039	25.444	0.056			
		corrected:	-13.426				

Appendix I: δ-Data, Day 0							
	$\delta^{13}C$		$\delta^{18}O$				
Samples	vs. PDB	Std. Dev.	vs. VSMOW	Std. Dev.	Corrected $\delta^{18}O$	Mean	Std. Dev.
SOIL							
0GCB10A	-4.468	0.021	36.839	0.059	-1.461	-2.831	2.490
0GCB10B	-4.232	0.031	32.595	0.048	-5.705		
0GCB10C	-4.313	0.045	36.972	0.039	-1.328		
0GCB10B dup	-4.286	0.035	32.94	0.083	-5.36		
0GCC10A	-4.402	0.031	31.336	0.015	-6.964	-7.205	0.367
0GCC10B	-5.02	0.018	30.673	0.066	-7.627		
0GCC10C	-4.378	0.049	31.276	0.056	-7.024		
0GTB10A	-4.46	0.039	33.134	0.052	-5.166	-4.356	3.523
0GTB10B	-4.446	0.032	30.896	0.048	-7.404		
0GTB10C	-4.631	0.013	37.801	0.044	-0.499		
0GTC10A	-4.533	0.031	31.552	0.026	-6.748	-6.714	0.033
0GTC10B	-4.764	0.038	31.617	0.059	-6.683		
0GTC10C	-4.563	0.02	31.59	0.07	-6.71		
0GCB30A	-4.407	0.044	46.128	0.069	7.738	3.817	4.401
0GCB30B	-4.448	0.027	37.446	0.044	-0.944		
0GCB30C	-4.44	0.041	43.046	0.065	4.656		
0GCC30A	-4.498	0.033	31.284	0.09	-7.106	-6.122	1.739
0GCC30B	-4.521	0.026	31.155	0.071	-7.145		
0GCC30C	-4.453	0.032	34.186	0.052	-4.114		
0GTB30A	-4.466	0.036	40.884	0.064	2.584	3.091	0.973
0GTB30B	-4.428	0.037	42.512	0.094	4.212		
0GTB30C	-4.503	0.03	40.776	0.062	2.476		
0GTB30B dup	-4.448	0.039	42.689	0.055	4.389		
0GTC30A	-5.242	0.058	33.054	0.074	-5.246	-4.340	1.601
0GTC30B	-4.659	0.034	35.809	0.073	-2.491		
0GTC30C	-4.779	0.033	33.017	0.072	-5.283		
0SCB10A	-4.391	0.031	32.46	0.078	-6.41	-5.053	1.658
0SCB10B	-4.483	0.042	35.185	0.04	-3.205		
0SCB10C	-4.457	0.023	32.846	0.073	-5.544		
0SCC10A	-4.515	0.049	34.519	0.066	-3.871	-5.141	1.113
0SCC10B	-4.464	0.02	32.439	0.07	-5.951		
0SCC10C	-4.683	0.054	32.79	0.065	-5.6		
0SCC10C dup	-4.618	0.023	32.925	0.062	-5.465		
0STB10A	-4.243	0.019	36.999	0.079	-1.391	-3.181	1.649
0STB10B	-4.318	0.043	33.752	0.032	-4.638		
0STB10C	-4.357	0.046	34.877	0.077	-3.513		
0STC10A	-4.307	0.035	33.857	0.027	-4.533	-4.377	1.782
0STC10B	-4.294	0.038	35.867	0.05	-2.523		
0STC10C	-4.383	0.035	32.314	0.055	-6.076		
0STC10C dup	-4.435	0.045	32.52	0.071	-5.87		
0STB30A	-4.592	0.041	42.002	0.058	3.612	4.906	1.142
0STB30B	-4.499	0.045	43.721	0.049	5.331		
0STB30C	-4.335	0.024	44.644	0.059	5.774		
0STC30A	-4.657	0.035	36.762	0.115	-1.628	-0.195	1.344
0STC30B	-4.777	0.019	39.427	0.055	1.037		
0STC30C	-4.564	0.027	38.876	0.04	0.006		
0SCB30A	-4.454	0.034	41.363	0.051	2.493	1.755	2.773
0SCB30B	-4.692	0.013	37.557	0.116	-1.313		
0SCB30C	-4.493	0.056	42.954	0.03	4.084		
0SCC30A	-4.664	0.017	35.732	0.018	-3.138	-1.322	3.747
0SCC30B	-4.403	0.053	41.857	0.058	2.987		
0SCC30C	-4.67	0.052	35.055	0.059	-3.815		

Appendix I: δ-Data, Day 2

*Date:	1/10/03		Temp:	38°C	Begin: 9am		
			Correction:	**37.65**	End: 6pm		
*Computer identifies as 01/09/2003 through 01/10/2003							
	δ^{13}C		δ^{18}O				
Standards	Delta-Mean	Std. Dev.	Delta-Mean	Std. Dev.			
Zero Enrich	-0.009	0.038	0.001	0.108			
Big Tank	-0.014	0.095	-0.04	0.131			
STD-STD	-3.545	0.02	24.81	0.088			
CO_2-8	-3.552	0.026	24.816	0.023			
RE53-02-46619	-4.152	0.023	24.682	0.045			
		corrected:	-12.968				
2/2/03	δ^{13}C		δ^{18}O		Temp:	36°C	Begin: 9am
Standards	Delta-Mean	Std. Dev.	Delta-Mean	Std. Dev.	Correction:	**38.02**	End: 5:30pm
Zero Enrich	-0.012	0.022	-0.064	0.072			
Big Tank	-0.004	0.03	-0.021	0.063			
STD-STD	-3.551	0.022	24.784	0.071			
CO_2-8	-3.539	0.042	24.822	0.056			
RE53-02-46619	-4.057	0.029	25.9	0.038			
		corrected:	-12.12				
	δ^{13}C		δ^{18}O				
Samples	vs. PDB	Std. Dev.	vs. VSMOW	Std. Dev.	Corrected δ^{18}O	Mean	Std. Dev.
SOIL							
2GCB10A	-4.559	0.02	39.568	0.023	1.548	-1.081	2.364
2GCB10B	-4.563	0.038	34.986	0.045	-3.034		
2GCB10C	-4.587	0.036	36.264	0.09	-1.756		
2GCC10A	-4.423	0.038	32.509	0.039	-5.511	-4.395	0.968
2GCC10B	-4.49	0.039	34.138	0.056	-3.882		
2GCC10C	-4.479	0.036	34.228	0.043	-3.792		
2GCC10A dup	-4.484	0.02	32.6	0.062	-5.42		
2GTB10A	-4.365	0.041	40.049	0.048	2.029	0.705	1.365
2GTB10B	-4.356	0.033	37.323	0.062	-0.697		
2GTB10C	-4.363	0.025	38.802	0.045	0.782		
2GTC10A	-4.413	0.046	33.676	0.016	-4.344	-4.357	0.221
2GTC10B	-4.51	0.018	33.877	0.051	-4.143		
2GTC10C	-4.514	0.017	33.435	0.049	-4.585		
2GTC10B dup	-4.514	0.018	33.764	0.025	-4.256		
2GCB30A	-4.533	0.041	41.779	0.04	4.129	0.658	3.464
2GCB30B	-4.416	0.04	34.852	0.061	-2.798		
2GCB30C	-4.29	0.05	38.294	0.02	0.644		
2GCC30A	-4.454	0.037	33.52	0.035	-4.13	-4.252	0.946
2GCC30B	-4.526	0.021	32.396	0.036	-5.254		
2GCC30C	-4.666	0.035	34.277	0.055	-3.373		
2GCC30A dup	-4.448	0.012	33.505	0.035	-4.145		
2GTB30A	-4.425	0.014	41.046	0.064	3.396	2.168	1.297
2GTB30B	-4.425	0.019	39.945	0.07	2.295		
2GTB30C	-4.455	0.018	38.462	0.053	0.812		

Appendix I: δ-Data, Day 2

	$\delta^{13}C$		$\delta^{18}O$				
Samples	vs. PDB	Std. Dev.	vs. VSMOW	Std. Dev.	Corrected $\delta^{18}O$	Mean	Std. Dev.
SOIL							
2GTC30A	-4.377	0.018	32.672	0.047	-4.978	-5.033	0.083
2GTC30B	-4.409	0.011	32.657	0.055	-4.993		
2GTC30C	-4.449	0.034	32.521	0.056	-5.129		
2GTC30B dup	-4.367	0.04	32.93	0.018	-4.72		
2SCB10A	-4.588	0.04	36.736	0.049	-1.284	-1.052	1.923
2SCB10B	-4.651	0.03	35.171	0.051	-2.849		
2SCB10C	-4.564	0.045	38.996	0.068	0.976		
2SCB10B dup	-4.578	0.03	35.367	0.06	-2.653		
2SCC10A	-4.567	0.017	35.193	0.024	-2.827	-2.691	0.681
2SCC10B	-4.564	0.047	36.067	0.035	-1.953		
2SCC10C	-4.533	0.045	34.726	0.034	-3.294		
2STB10A	-4.499	0.035	37.933	0.039	-0.087	0.878	2.322
2STB10B	-4.574	0.022	41.547	0.061	3.527		
2STB10C	-4.508	0.044	37.213	0.039	-0.807		
2STB10C dup	-4.493	0.036	37.078	0.047	-0.942		
2STC10A	-4.523	0.017	37.954	0.025	-0.066	-2.259	1.926
2STC10B	-4.487	0.039	34.347	0.026	-3.673		
2STC10C	-4.512	0.018	34.982	0.07	-3.038		
2STB30A	-4.542	0.036	42.536	0.021	4.886	4.915	0.473
2STB30B	-4.471	0.018	43.052	0.03	5.402		
2STB30C	-4.606	0.033	42.108	0.042	4.458		
2STB30A dup	-4.556	0.035	42.764	0.055	5.114		
2STC30A	-4.55	0.029	38.103	0.058	0.453	-0.805	2.516
2STC30B	-4.56	0.022	33.948	0.039	-3.702		
2STC30C	-4.568	0.016	38.485	0.035	0.835		
2SCB30A	-4.298	0.032	46.433	0.081	8.413	5.547	4.829
2SCB30B	-4.468	0.028	37.622	0.065	-0.028		
2SCB30C	-4.5	0.049	45.907	0.06	8.257		
2SCC30A	-4.541	0.033	37.685	0.037	0.035	-0.079	0.182
2SCC30B	-4.527	0.034	37.303	0.041	-0.347		
2SCC30C	-4.578	0.048	37.688	0.057	0.038		
2SCC30C dup	-4.577	0.013	37.608	0.048	-0.042		

Appendix I: δ-Data, Day 6

*Computer identifies 10/29,30 & 11/12,13/2003								
10/29/03	$\delta^{13}C$		$\delta^{18}O$		Temp:	31.5°C	Begin:11am	
Standards	Delta-Mean	Std. Dev.	Delta-Mean	Std. Dev.	Correction:	**38.87**	End: 7pm	
Zero Enrich	0.007	0.022	-0.01	0.045				
Big Tank	0.005	0.024	-0.011	0.092				
STD-STD	-3.521	0.01	24.718	0.042				
CO_2-8	-3.535	0.019	24.765	0.061				
RE53-02-46619	-4.24	0.039	25.444	0.056				
		corrected:	-13.43					
11/12/03	$\delta^{13}C$		$\delta^{18}O$		Temp:	33°C	Begin:11am	
Standards	Delta-Mean	Std. Dev.	Delta-Mean	Std. Dev.	Correction:	**38.58**	End: 6:30pm	
Zero Enrich	0.021	0.032	0.04	0.087				
Big Tank	0.006	0.024	0.033	0.064				
STD-STD	-3.525	0.043	24.796	0.059				
CO_2-8	-3.545	0.039	24.786	0.027				
RE53-02-46619	-4.291	0.017	25.793	0.009				
		corrected:	-12.79					

Appendix I: δ-Data, Day 6								
*2/15/2003	δ^2H			H_3	Correction Equation:			
Standards	Delta-Mean	Std. Dev.		50.839	1.0112*X + 5.13			
Zero Enrich	-0.663	0.148						
Zero Enrich dup	-0.802	0.326			*Computer identifies 02/14-15/1992			
STD-STD	-52.254	0.249						
STD-STD dup	-52.314	0.084						
NM-2	-100.991	0.2						
*2/16/2003	δ^2H			H_3	Correction Equation:			
Standards	Delta-Mean	Std. Dev.		51.686	1.0112*X + 5.13			
Zero Enrich	-0.552	0.398						
Zero Enrich dup	-0.297	0.167			*Computer identifies 02/15-16/1992			
STD-STD	-51.255	0.144						
STD-STD dup	-51.344	0.346						
NM-2	-99.842	0.074						
*2/19/2003	δ^2H			H_3	Correction Equation:			
Standards	Delta-Mean	Std. Dev.		51.360	1.0112*X + 5.13			
Zero Enrich	-0.579	0.214						
Zero Enrich dup	-0.238	0.108			*Computer identifies 02/19-20/1992			
STD-STD	-51.869	0.625						
STD-STD dup	-52.375	0.454						
NM-2	-100.94	0.186						
REINTRODUCE								
Zero Enrich	-0.898	0.085						
STD-STD	-52.343	0.219						
2/21/03	δ^2H			H_3	Correction Equation:			
Standards	Delta-Mean	Std. Dev.		49.102	1.0112*X + 5.13			
Zero Enrich	0.022	0.192						
Zero Enrich dup	-0.199	0.258						
STD-STD	-52.185	0.286						
STD-STD dup	-52.912	0.236						
BEGAN AFTER	TALON NEWTON							
2/23/03	δ^2H			H_3	Correction Equation:			
Standards	Delta-Mean	Std. Dev.		50.691	1.0112*X + 5.13			
Zero Enrich	-2.208	2.224						
Zero Enrich dup	-0.348	0.228						
STD-STD	-51.859	0.349						
STD-STD dup	-51.935	0.112						
NM-2	-96.935	0.252						
BEGAN AFTER	TALON NEWTON							
New Zn								
NM-2	-98.308	0.21						

Appendix I: δ-Data, Day 6								
Samples	δ^2H vs. SMOW	Std. Dev.	Corrected δ^2H	Mean	Std. Dev.	ΔP	δ correction	Final δ^2H
6GCB10A	-32.477	0.523	-27.711	-29.917	3.037	-0.025	-4.528	-32.239
6GCB10B	-33.414	0.383	-28.658			-0.019	-3.76732	-32.426
6GCB10C	-38.084	0.328	-33.381			-0.034	-5.66902	-39.050
6GCC10A	-47.133	0.666	-42.531	-47.550	5.056	-0.039	-6.30292	-48.834
6GCC10B	-52.025	0.509	-47.478			-0.049	-7.57072	-55.048
6GCC10C	-57.133	0.133	-52.643			-0.007	-2.24596	-54.889
6GCB30A	-30.709	0.134	-25.923	-30.585	4.041	0	-1.3585	-27.281
6GCB30B	-37.467	0.167	-32.757			0	-1.3585	-34.115
6GCB30C	-37.783	0.162	-33.076			0.002	-1.10494	-34.181
6GCC30A	-56.029	0.277	-51.527	-53.053	4.102	-0.002	-1.61206	-53.139
6GCC30B	-54.453	0.193	-49.933			-0.002	-1.61206	-51.545
6GCC30C	-62.134	0.121	-57.700			0	-1.3585	-59.058
6GTB30A	-37.978	0.251	-33.273	-36.719	3.919	0.005	-0.7246	-33.998
6GTB30B	-40.577	0.247	-35.901			-0.005	-1.9924	-37.894
6GTB30C	-45.602	0.569	-40.983			-0.091	-12.89548	-53.878
6GTC30A	-53.807	0.186	-49.280	-48.065	1.916	0	-1.3585	-50.638
6GTC30B	-53.588	0.227	-49.058			0.002	-1.10494	-50.163
6GTC30C	-50.421	0.179	-45.856			0.009	-0.21748	-46.073
6GTB10A	-28.134	0.188	-23.319	-29.824	6.467	0.01	-0.0907	-23.410
6GTB10B	-34.642	0.393	-29.900			0.005	-0.7246	-30.625
6GTB10C	-40.925	0.235	-36.253			0.005	-0.7246	-36.978
6GTC10A	-47.532	0.142	-42.934	-42.190	2.765	0.005	-0.7246	-43.659
6GTC10B	-43.769	0.235	-39.129			0.005	-0.7246	-39.854
6GTC10C	-49.088	0.189	-44.508			0.002	-1.10494	-45.613
6GTC10A dup	-48.001	0.163	-43.409			0.002	-1.10494	-44.514
6SCB10A	-33.93	0.189	-29.180	-36.982	9.511	0.012	0.16286	-29.017
6SCB10B	-38.883	0.294	-34.188			0.019	1.05032	-33.138
6SCB10C	-52.123	0.076	-47.577			0	-1.3585	-48.935
6SCC10A	-52.486	0.254	-47.944	-43.324	4.288	0.012	0.16286	-47.781
6SCC10B	-44.106	0.161	-39.470			0.01	-0.0907	-39.561
6SCC10C	-47.161	0.249	-42.559			0.02	1.1771	-41.382
6STB10A	-42.595	0.249	-37.942	-35.666	2.939	0	-1.3585	-39.301
6STB10B	-41.374	0.304	-36.707			0.005	-0.7246	-37.432
6STB10C	-37.062	0.204	-32.347			0.007	-0.47104	-32.818
6STB10B dup	-42.207	0.222	-37.550			0.005	-0.7246	-38.274
6STC10A	-37.746	0.227	-33.039	-31.137	2.616	0.007	-0.47104	-33.510
6STC10B	-32.915	0.268	-28.154			0.002	-1.10494	-29.259
6STC10C	-36.936	0.365	-32.220			0.007	-0.47104	-32.691
6STB30A	-34.215	0.254	-29.468	-31.585	2.565	0	-1.3585	-30.827
6STB30B	-39.129	0.282	-34.437			-0.002	-1.61206	-36.049
6STB30C	-35.58	0.287	-30.848			-0.012	-2.87986	-33.728
6STC30A	-48.559	0.128	-43.973	-38.532	4.938	-0.015	-3.2602	-47.233
6STC30B	-39.028	0.202	-34.335			-0.017	-3.51376	-37.849
6STC30C	-41.948	0.288	-37.288			-0.022	-4.14766	-41.435
6STC30C dup	-41.26	0.414	-36.592			-0.024	-4.40122	-40.993
6SCB30A	-32.396	0.219	-27.629			0.012	0.16286	-27.466
6SCB30B	-37.722	0.268	-33.014			0.017	0.79676	-32.218
6SCB30C	-37.935	0.293	-33.230			0.014	0.41642	-32.813
6SCC30A	-47.07	0.277	-42.467	-38.738	3.298	-0.005	-1.9924	-44.460
6SCC30B	-40.878	0.315	-36.206			0.003	-0.97816	-37.184
6SCC30C	-42.198	0.218	-37.541			0	-1.3585	-38.899

This thesis is accepted on behalf of the
Faculty of the Institute by the following committee:

Advisor

Date

I release this document to the New Mexico Institute of Mining and Technology.

Student's Signature 01/08/04 Date